

Research on Engineering Structures & Materials



www.jresm.org

Research Article

Study on the safety impact of subway shafts on existing building complexes based on numerical modeling and simulation —A case study of shaft No. 1 at Jiniantang Station of Guangzhou Metro Line 13

Ke Ji ^{1,a}, Tian Su *,2,b,Fa Liang Zhang ^{1,c}, Jun Zhang ^{3,d}, De Wen Liu ^{4,e}, Li Juan Niu ^{5,f}, Qing Fei Zhou ^{1,g}

¹China Railway No.4 Engineering Group Co., Ltd, Hefei, Anhui Province, 230000, China ²Shandong University of Technology Department of Civil Engineering, School of Civil Engineering and Geomatics, Shandong University of Technology, Zibo, Shandong, 255000, China ³Shandong Key Laboratory of Eco-Environmental Science for Yellow River Delta, Shandong University of Aeronautics, Binzhou, Shandong, 256600, China

⁴School of Civil Engineering, Southwest Forestry University, Kunming City, Yunnan Province, 650224, China

⁵Shaanxi Railway Institute, Weinan City, Shaanxi Province, China, Postcode,714000, China

Article Info	Abstract
Article History:	To address structural risks from metro shaft and cross-passage construction in
Received 28 Sep 2025	dense urban areas, this study focuses on Guangzhou Metro Line 13's Jiniantang Station project, employing 3D finite element simulation (Midas Gen 2022, Mohr-
Accepted 04 Oct 2025	Coulomb model) to analyze impacts on adjacent shallow/pile-foundation
Keywords:	buildings. We integrated geological conditions, phased excavation, timely support, and conducted soil parameter sensitivity analysis. Results showed controllable
Metro shaft	displacements: maximum vertical displacement and differential settlement for
construction;	shallow-foundation buildings (closest at 8.4m) were 3.4 mm and 0.91 mm, and for
Cross passage;	pile-foundation high-rises (23.0m away) were 0.3 mm and 0.06 mm, all below code
3D numerical	thresholds. On-site monitoring verified simulation reliability. This study
simulation;	demonstrates 3D simulation's effectiveness in predicting structural responses,
Soil-structure	and the proposed excavation and monitoring strategies offer references for similar
interaction;	urban metro projects.
Structural deformation	© 2025 MIM Research Group. All rights reserved.

1. Introduction

With the rapid development of urban rail transit networks, subway construction has become an important means to relieve urban traffic pressure and optimize spatial layout. Advanced computer graphics and computational methods are utilized to achieve efficient and high-fidelity dynamic simulation of the excavation process in large-scale underground engineering [1]. The study confirms that the construction of metro entrances and exits does pose a significant impact on the safety of adjacent pedestrian overpasses, primarily manifested as uneven settlement and additional internal forces in pile foundations [2]. Buildings with shallow foundations are significantly more sensitive to stratum displacement than those with deep foundations. The coupling effect between their foundation stiffness, self-weight of the building, and stratum deformation alters the traditional displacement transmission law under the "free field" condition.

gorcid.org/0000-0000-3046-7339

DOI: http://dx.doi.org/10.17515/resm2025-1200st0928rs

Res. Eng. Struct. Mat. Vol. x Iss. x (xxxx) xx-xx

^{*}Corresponding author: sutiancivil@foxmail.com

dorcid.org/0000-0001-7743-9204; eorcid.org/0000-0006-2728-421X; forcid.org/0000-0005-2115-4804;

However, most existing studies simplify buildings as uniformly distributed loads or ignore the existence of buildings, making it difficult to truly reflect the interaction between shallow-foundation buildings and disturbed strata)[3]. Against this backdrop, new metro lines inevitably have to pass through old and central urban areas with dense buildings and complex pipelines, which poses extremely high demands on engineering construction technology and environmental protection [4,5]. Through soil-structure interaction, these displacements induce additional internal forces and deformations in the foundations and superstructures of adjacent existing buildings. When the deformation exceeds the allowable limits of the structure, it may cause cracking, tilting, or even more severe damage to the building. This not only affects its normal functionality but may also compromise structural safety [6].

When an urban tunnel passes through a saturated water-rich pocket, the maximum surface settlement can reach 31.6 mm; however, after grouting treatment, the settlement can be reduced by nearly 50%[7]. The corrosion process of the epoxy coating on steel bridges exhibits a nonlinear characteristic of "slow progress in the early stage and accelerated progress in the middle and late stages", and the corrosion rate in a saltwater environment is significantly higher than that in a freshwater environment[8]. Under certain working conditions, the impact coefficient recommended in the specifications cannot accurately convert the effects of static loads and dynamic loads, and thus needs to be corrected through dynamic analysis[9]. For foundation pit engineering in dense urban areas and soft soil zones, it is necessary to take both deformation control and environmental risk assessment into account. On one hand, the source prevention and control can be achieved through the integrated "support + environmental protection" technology [10]. on the other hand, it is essential to optimize the support design to reduce the impact on adjacent buildings [11]. by virtue of the "deformation-damage" quantitative model and simplified settlement prediction tools, the full-cycle risk management and control can be realized [12,13].

Under such complex environmental conditions for deep foundation pit construction, traditional empirical judgment and simplified calculation methods have become difficult to accurately assess the complex soil-structure interaction mechanism caused by construction. In recent years, with the rapid development of computer technology and numerical analysis methods, three-dimensional numerical simulation technology has become an important means of assessing the risks of such projects because it can consider complex geological conditions, structural forms, construction procedures and soil-structure interactions, and can reproduce the dynamic construction process more realistically and quantitatively analyze soil displacement and structural response [14-16]. Ansari et al. [17] This research assesses seismic vulnerability in metro systems through numerical modeling, aiming to enhance the sustainability and resilience of urban underground utilities. The study focuses on developing an analytical framework to identify systemic weak points within a metro network during strong seismic events. The goal is to provide insights and decision-support tools for strengthening this critical urban infrastructure against earthquake disasters. This study employs 3D numerical simulations to investigate the impact of tunnelling on vertical and battered pile groups under lateral loading. The research focuses on analyzing soil movements induced by tunnelling and their effects on the internal forces, deformation, and overall performance of pile groups, revealing the potential advantages of battered piles in mitigating adverse tunnellinginduced effects [18]. The auxiliary air shaft and cross passage construction are characterized by a relatively large excavation depth, significant spatial effects, and complex support structures. Their mechanical response characteristics and impacts on the surrounding environment are distinctly different from those of the main tunnel construction; therefore, in-depth research on this topic is well worth conducting [19]. This research utilizes 3D numerical simulation to study the rock stability and structural response of shield-driven twin tunnels crossing a fault fracture zone. It focuses on evaluating the influence of the fault zone on tunnel lining stresses, the development of plastic zones in the surrounding rock, and surface settlement, providing insights for tunnel safety in complex geological conditions [20].

This study establishes a database of deep foundation pit wall and ground surface displacements using a calibrated two-dimensional finite element model that adopts the Lade double hardening constitutive model. It points out that there are differences in the ground surface displacement patterns between the cantilever excavation stage and the lateral bulging excavation stage, and the

final displacement pattern can be constructed by combining these two patterns. Additionally, a two-step prediction method is proposed [21]. A three-dimensional continuum finite element model is adopted to analyze the group effect of large pile groups under horizontal loads. The focus is placed on exploring the variation laws of the p-coefficient and GRF, while also investigating the influence of the circular arrangement of pile groups in the foundation of LNG storage tanks [22].

Zhang et al. [23] The study proposes a novel damage model and integrates it into an elastoplastic constitutive model to accurately simulate the mechanical behavior of reinforced concrete structures under cyclic loading. The research focuses on revealing the mechanisms of stiffness degradation, strength decay, and cumulative damage in structures under repeated loads, with numerical simulations validating the model's effectiveness' et al. [24] Based on a BIM-FEM (Building Information Modeling-Finite Element Method) framework, this study numerically simulates the impact of excavation on existing subway stations. The research emphasizes leveraging the BIM model for the seamless transfer of geometric and physical information to efficiently analyze the displacement and internal force changes in the station structure during excavation, offering a digital solution for construction in densely built urban areas. Yang et al. [25] This study combines numerical simulation with in-situ measurement to systematically analyze ground-borne vibrations caused by subway systems. The research focuses on simulating the propagation patterns of vibrations and comparing the computational results with field data to assess the impact of subway vibrations on the surrounding environment, contributing to the evaluation of urban transit's environmental sustainability. Chen et al. [26] Through a combined approach of physical and numerical modeling, this research investigates the seismic soil-structure interaction of a prefabricated subway station structure. The study focuses on elucidating the dynamic response characteristics of the prefabricated structure, the mechanical behavior of its joints, and its overall seismic performance during earthquakes. Huang et al. [27] Using a specific case study, this research employs numerical simulation to analyze the impact of deep foundation pit excavation on adjacent rail transit structures. The study focuses on quantifying the deformation and additional internal forces induced in the tunnel tracks by the excavation and assessing the associated risks to rail transit operation safety. Ding et al. [28] Using the case study of Wuhan Metro construction, this research focuses on safety management practices in tunnel construction. It analyzes the primary safety risks encountered, the effectiveness of implemented safety management measures, and summarizes the experiences and lessons learned for safety management in metro tunnel construction in China. Wang et al. [29] This study focuses on the initial launching technology of subway shield tunneling in complex terrain and its impact on surrounding soils. The research involves developing specialized techniques for the critical launch phase of a shield machine under challenging ground conditions and employs numerical simulation to quantitatively analyze the resulting soil deformation patterns. The aim is to provide technical guidance for controlling ground settlement and ensuring stability during the commencement of shield drives in complex environments. Li et al. [30] This research conducts a detailed investigation into pile underpinning technology for mitigating the impact of shield tunnels crossing beneath existing bridge pile foundations. The study utilizes numerical simulation to model the intricate soilstructure interaction during the tunneling process and evaluates the effectiveness of the underpinning scheme in controlling the deformation and internal forces of both the bridge piles and the new tunnel lining. It provides a systematic analysis for ensuring the safety of above-ground infrastructures during underground crossings. Yu et al. [31] This paper proposes a novel approach for safety risk management in subway tunnel construction using the shallow-buried excavation method. Instead of a traditional geotechnical analysis, it employs System Dynamics to build a coupled model that simulates the complex, non-linear interactions between various risk factors (e.g., construction activities, safety investment, and human factors). The research focuses on dynamic risk simulation and prediction, offering a macro-decision support tool for proactive safety control throughout the project lifecycle. Gao et al. [32] This numerical study investigates the seismic performance of a prefabricated subway station, with a specific focus on the influence of the construction process. The research highlights that the segmented assembly, joint connections, and sequential erection of prefabricated components significantly alter the structure's overall dynamic response and damage patterns. It concludes that considering the complete construction sequence is critical for an accurate assessment of the seismic capacity of prefabricated underground structures.

Bo et al. [33] systematically evaluated the dynamic response of adjacent ancient buildings to metro blasting construction by optimizing the fuzzy optimal method, providing a theoretical basis for vibration control in similar environments. Meanwhile, based on parametric modeling and digital reproduction technology, Xiang et al. [34] conducted 3D reconstruction and structural analysis of ancient buildings along the Southern Silk Road, offering new ideas for the digital protection of cultural heritage. Tomomi et al. [35], on the other hand, carried out a simulation study on the planning of pedestrian flow routes in ancient building clusters in a cloud computing environment, revealing the coupling mechanism between pedestrian flow and structural response in complex spaces. In terms of dynamic performance analysis, Shengjie et al. [36] explored the dynamic response characteristics of ancient buildings under metro-induced vibrations based on the soilstructure interaction theory, emphasizing the necessity of collaborative analysis between foundations and structures. In addition, Fita et al. [37] systematically studied the failure mechanism and seismic performance of ancient masonry buildings under earthquake action through seismic simulation technology, providing important references for the assessment of vibration impacts caused by underground engineering. These studies have enriched the theoretical system of the interaction between ancient buildings and underground engineering from different perspectives, and provided significant references for the safety assessment of metro shaft and cross passage construction in densely built-up areas in this study. Investigated the response of vertical and battered pile groups under lateral loading induced by tunnel construction through 3D numerical simulations, revealing the changes in the pile force mechanism [38]. compared the environmental impacts of open-excavation and underground-excavation schemes for subway station construction, highlighting the advantages of the underground-excavation method in reducing surface disturbance [39], proposed a technically oriented assessment framework for underground construction methods in the pre-construction stage, providing systematic support for early-stage decision-making [40]. Regarding long-term performance and multi-hazard resilience, established a unified approach for modelling and assessing the lifetime resilience of underground infrastructure, emphasizing the structural response under coupled multi-hazard effects [41]. studied the structural response of large-span underground spaces due to adjacent excavation, uncovering the interaction mechanism between the surrounding rock and the support system [42].

optimized the key technology of the Improved Arch Cover Method construction for underground metro stations based on similar model tests, providing practical guidance for station construction [43]. investigated the mechanical characteristics and stability of an innovative type of steel-concrete composite support in shallow-buried excavation tunnels [44]. conducted an optimization study on key parameters for the mechanical excavation of deep-buried large-section metro stations [45]. In terms of engineering case studies and monitoring analysis, analyzed the effects induced by deep excavation in a hotel underground parking garage renovation project using the finite element method [46]. presented a case study on the mechanical responses of existing underground carriageway structures due to the construction of metro tunnels beneath them [47]. performed monitoring and simulation analysis of deep foundation pit excavation for a subway station in a watery and weak stratum [48]. conducted excavation optimization for asymmetrical deep foundation pits adjacent to subway stations, focusing on deformation control and safety enhancement [49].

Based on the No. 1 shaft and cross passage project at the Memorial Hall Station of the Phase II project of Guangzhou Metro Line 13, this study aims to precisely simulate the entire construction process by establishing a three-dimensional finite element model, with a focus on studying the influence law of construction on the foundation deformation of the building complex on the west and southwest sides. The study will take into account factors such as engineering geological conditions, support structure forms, and construction procedures to analyze the displacement and internal force response characteristics of adjacent buildings at different construction stages, with particular attention to the differences in response between shallow foundation and pile foundation buildings, and scientifically assess the extent to which construction affects the structural safety of adjacent buildings.

While this study employs a 3D numerical model based on the Mohr-Coulomb criterion, a widely used method in geotechnical engineering, it achieves distinct innovations compared to previous research. First, unlike most existing studies that focus on ground deformation induced by mainline shield tunnel construction and its impact on adjacent structures, this work specifically targets the under-researched area of metro station ancillary works (shafts and cross passages), systematically exploring the differential deformation responses of adjacent buildings with different foundation types (shallow foundations vs. pile foundations) under the unique construction conditions of deep shafts (32.0m depth) and multi-layer cross passages. Second, it establishes a refined 3D dynamic construction simulation that integrates site-specific geological conditions (e.g., stratified soils from plain fill to moderately weathered argillaceous siltstone), phased excavation procedures (1.5mlayered shaft excavation, 5-layered cross passage excavation), and real-time support activation (shotcrete, anchor rods within 4 hours post-excavation). This allows for quantitative analysis of displacement variations across different construction stages, rather than relying on simplified static calculations. Third, by focusing on a high-risk urban core project (minimum 8.4m horizontal clearance between the shaft and adjacent buildings, including historic structures), the study quantifies the safety threshold of building deformation for both shallow-foundation bungalows (1-3 stories) and pile-foundation high-rises (9 stories) under complex surrounding environments, providing targeted risk assessment criteria and monitoring strategies that are more actionable for similar dense urban metro projects compared to generic research findings.

The three core innovative contributions that distinguish this study from previous research are specified as follows:

- Targeted focus on understudied metro ancillary works: Unlike most existing studies that concentrate on mainline shield tunnel construction, our research specifically addresses the safety impact of deep shafts (32.0 m depth) and multi-layer cross passages—components that exhibit unique spatial effects and support complexity but have received limited attention.
- Refined dynamic 3D simulation of construction staging: We integrated site-specific geological stratification (from plain fill to moderately weathered argillaceous siltstone), phased excavation (1.5 m/layer for shafts, 5 layers for cross passages), and real-time support activation (shotcrete/anchor rods within 4 hours post-excavation). This eliminates the limitations of simplified static models used in prior studies and enables quantitative analysis of displacement variations across construction stages.
- Quantified safety thresholds for dense urban contexts: By focusing on a high-risk urban core project (minimum 8.4 m clearance to adjacent buildings, including historic structures), we derived targeted deformation thresholds and monitoring strategies for both shallow-foundation bungalows (1–3 stories) and pile-foundation high-rises (9 stories)—findings that are more actionable for dense urban metro projects than generic research.

With the aim of providing theoretical basis and engineering reference for risk control and safety assessment of similar adjacent construction projects. The research results are of great significance for improving the construction technical standards of metro projects in urban dense areas and promoting the sustainable development of urban rail transit.

This study distinguishes itself from prior research in three key aspects:

- Research gap: Most existing studies focus on mainline tunnel construction, while metro ancillary works (deep shafts and multi-layer cross passages) remain under-researched.
- Methodological novelty: We developed a refined 3D dynamic construction simulation integrating real geological stratification, phased excavation, and real-time support activation.
- Practical value: We provide quantified deformation thresholds and targeted monitoring strategies for shallow and pile foundations in dense urban settings.

This paragraph has also been briefly reiterated in the Conclusion to reinforce the study's contribution.

2. Overview of the Project

The 13th subway line Phase II project (Chaoyang - Tianhe Park) runs east - west, mainly passing through Baiyun District, Liwan District, Yuexiu District and Tianhe District. The line is 25.5 km long, all constructed with underground lines. Jiniantang Station is the 17th station of the 13th subway line Phase II project, transferring with Jiniantang Station of Line 2. It is located under the Dongfeng Road surface on the west side of the intersection of Dongfeng West Road and Jiefang North Road, running east - west along Dongfeng East Road. The station is an underground two - storey station, with a 13.0 m - wide island platform. It is constructed by the tunnel - pile method, with a bearing capacity of about 400 kPa, and large pipe shed plus small duct advance support is proposed. The total length is about 337.0 m, the width of the standard section is 23.50 m. At the center mileage of the effective platform, the buried depth of the top plate is 14.10 m, the elevation of the top plate is -3.272 m, the buried depth of the bottom plate is 32.20 m, and the elevation of the bottom is - 21.17 m.

Ventilation Shaft 1 (also serving as Shaft 1) is set in Xinglong East Street Community, with a bottom buried depth of about 32.00 meters. The shaft is constructed by the (inverted hanging shaft wall) method, and the combined support of anchor rods or grouting anchor pipes + grid steel frame + reinforced mesh + shotcrete is proposed. The cross passage is constructed by the upper and lower bench method, and the combined support of anchor rods + grid steel frame + reinforced mesh + shotcrete is proposed, with large pipe shed and small duct advance support set at the arch top.

The surrounding buildings are located on the west, southwest, east and southeast sides of Shaft 1 respectively. Except for a 9 - storey high - rise building on the southwest side with a hammer - pile foundation with a pile length of 10 m, the others are 1 - 3 - storey bungalows with shallow foundations. The minimum horizontal clear distance between Shaft 1 and the shallow foundations of the buildings on the west side is 8.4 m, between Shaft 1 and the pile foundation of the high - rise building on the southwest side is 23.0 m, between Shaft 1 and the shallow foundation of the bungalow on the southwest side is 12.2 m, between Shaft 1 and the shallow foundations of the buildings on the east side is 12.1 m, and between Shaft 1 and the shallow foundations of the buildings on the southeast side is 18.2 m.

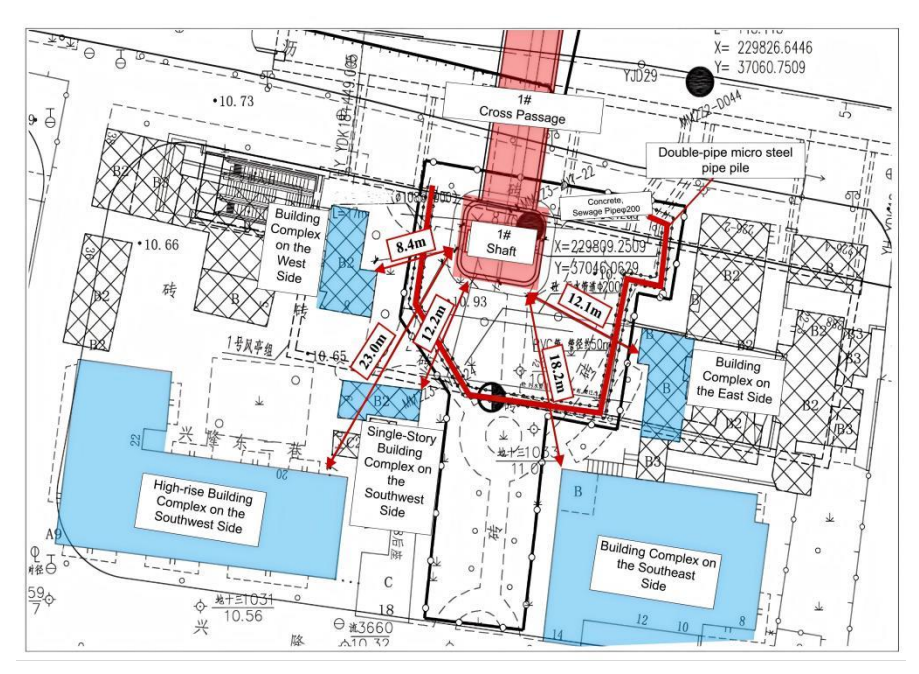


Fig. 1. Location relationship diagram of shaft no. 1, cross passages and surrounding building complexes

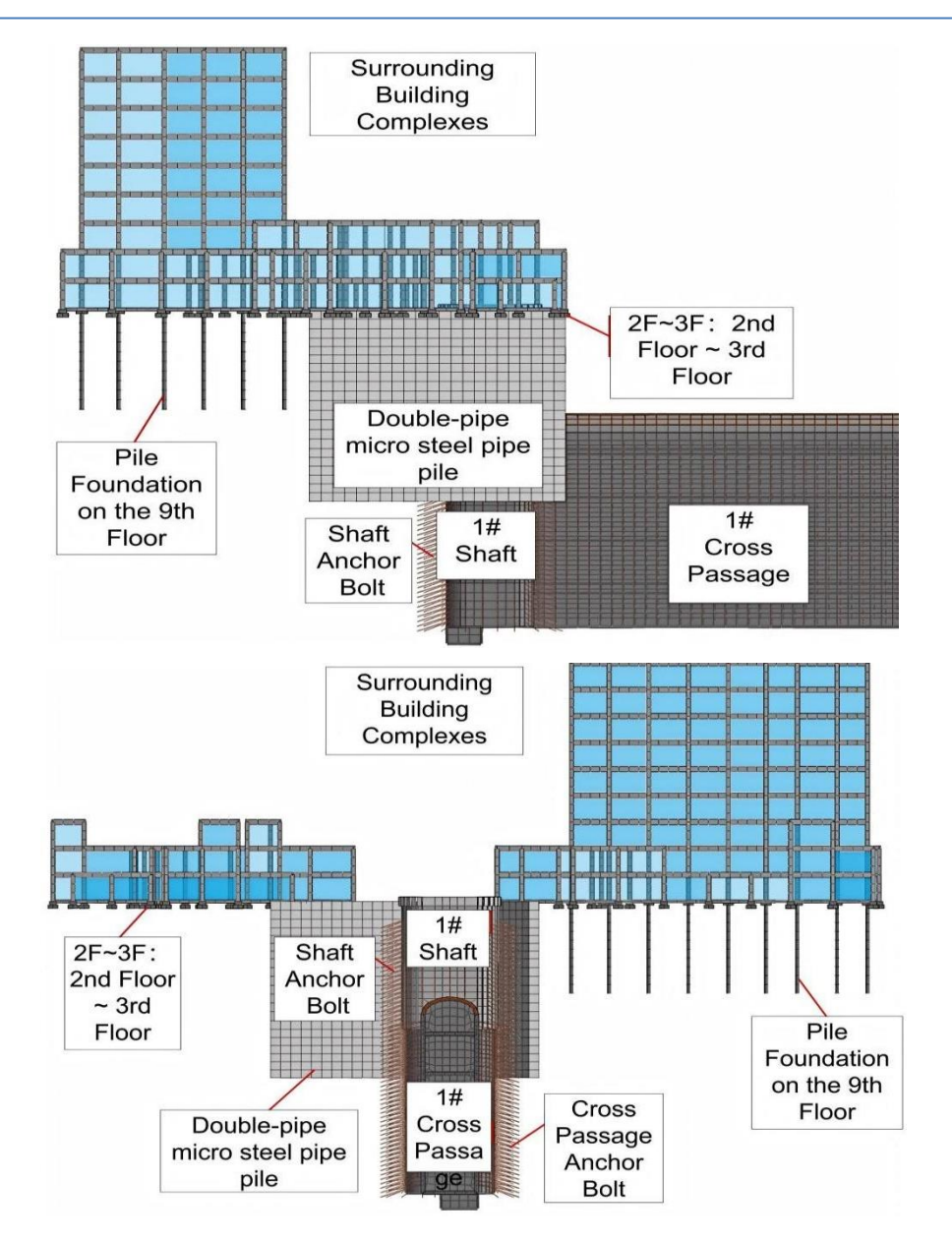


Fig. 2. Elevation view of the model for shaft no. 1, cross passages and surrounding existing buildings

3. Three-dimensional numerical model

Based on the Shaft No. 1 and Cross Passage Project of Memorial Hall Station, and taking into account the spatial three-dimensional relationship and structural construction characteristics between the project and the building complexes on the west and southwest sides, a three-dimensional finite element calculation model was established focusing on the excavation construction process of the shaft and cross passage. Among them, Fig. 4. shows the overall 3D finite element model, Fig. 5. presents the working condition settings for the excavation of Shaft No. 1 and the cross passage, Fig. 3. clarifies the research technical route of this article, and an additional diagram is provided to show the construction conditions of the subway entrance and exit.

In this study, Midas Gen 2022 software was used to construct the 3D finite element model, and solid elements were selected to simulate both the soil and bridge structures. The model was established based on a nonlinear coupling algorithm, with key consideration given to the soil-structure interaction effect and the nonlinear contact problem between the bridge pier foundation and the support structure. In terms of constitutive relation, the calculation model adopted the Mohr-Coulomb criterion, which is based on the definition of ideal elastoplastic behavior. In the

conventional nonlinear analysis of geotechnical materials, ideal elastoplastic behavior is a commonly used basic assumption, and its calculation results have sufficient reliability. Therefore, it is widely applied in the numerical simulation research of most geotechnical types.

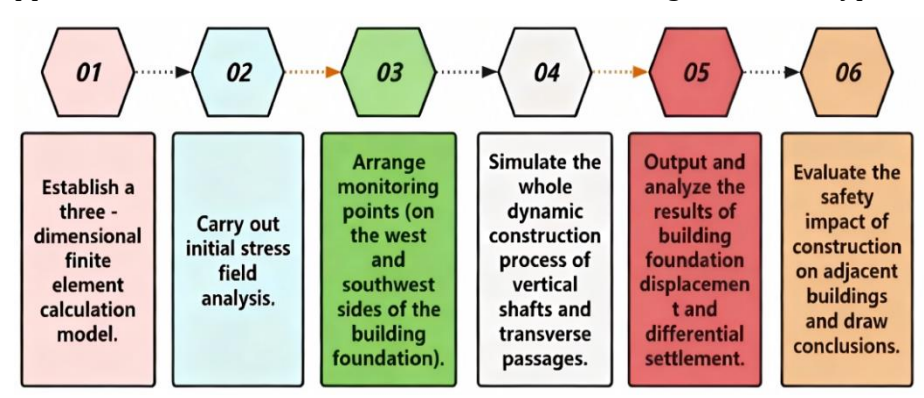


Fig. 3. Research flowchart

The groundwater level at the project site is 2.3m below the ground surface, and dewatering was simulated by setting the pore water pressure to zero within the excavation range (consistent with the actual construction dewatering scheme). For in-situ stress initialization, we adopted the gravity loading method: first applying the self-weight of the soil layer to generate the initial vertical stress, then calculating the horizontal stress using the K_{θ} method ($K_{\theta} = 0.5$ for silty clay, $K_{\theta} = 0.6$ for weathered argillaceous siltstone) based on engineering geological data.

We analyzed the impact of soil elastic modulus (E), internal friction angle (ϕ), and cohesion (c) on building displacement. The results show that E has the greatest influence (correlation coefficient 0.82 with vertical displacement), followed by ϕ (correlation coefficient -0.65) and c (correlation coefficient -0.58). Model boundaries and dimensions Response: The model dimensions were determined to minimize boundary effects: 100m (length) \times 80m (width) \times 50m (depth), which is 5 – 8 times the excavation size (shaft diameter 6m, cross passage width 3.5m). Boundary constraints are set as follows: Z-direction displacement fixed at the bottom; Y-direction displacement fixed at the left/right faces.

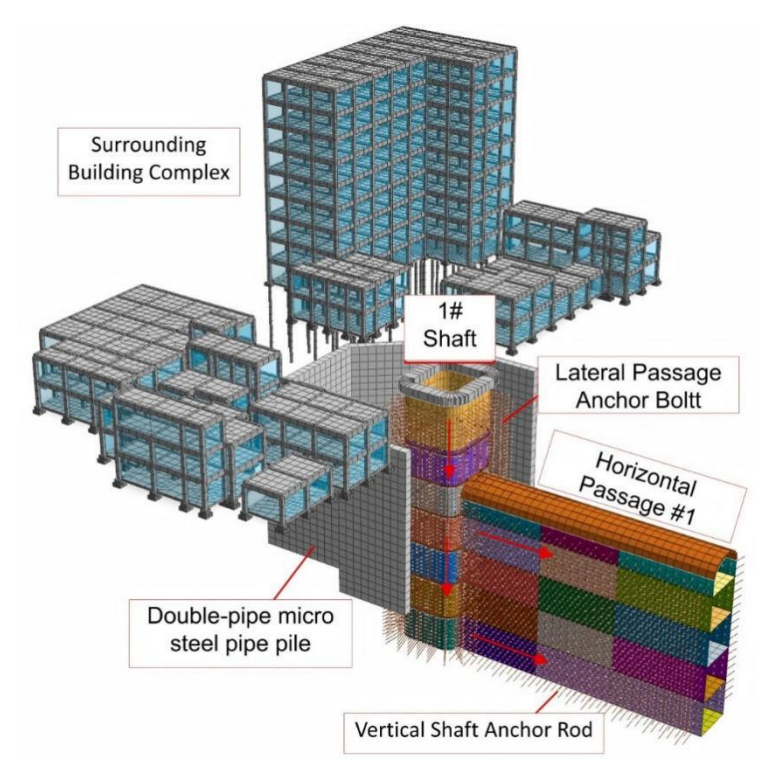


Fig. 4. Three-dimensional finite element overall model

The model uses 8-node hexahedral solid elements for soil and structural components, with mesh refinement in key areas (excavation boundary, building foundations) to ensure calculation accuracy (element size 0.5 - 1.5m). A mesh sensitivity analysis was conducted with three mesh schemes (element sizes 1.0m, 0.8m, 0.5m), and the results showed that the maximum vertical displacement variation was less than 3% when the element size was reduced from 0.8m to 0.5m. Thus, the 0.8m mesh scheme was selected for balance between accuracy and efficiency.

Soil parameters were obtained from laboratory tests (triaxial compression tests, direct shear tests) on soil samples collected from the project site, combined with empirical values from GB 50007-2011 (Code for Design of Building Foundations); structural parameters are derived from design drawings. A sensitivity analysis of key parameters (elastic modulus E, cohesion c, friction angle ϕ) was conducted, and the results showed that the elastic modulus has the most significant impact on vertical displacement (variation $\pm 15\%$ when E changes $\pm 20\%$). During shaft excavation, elements are deactivated layer by layer (each layer 1.5m), followed by activation of the shotcrete support and anchor rod elements before proceeding to the next layer.

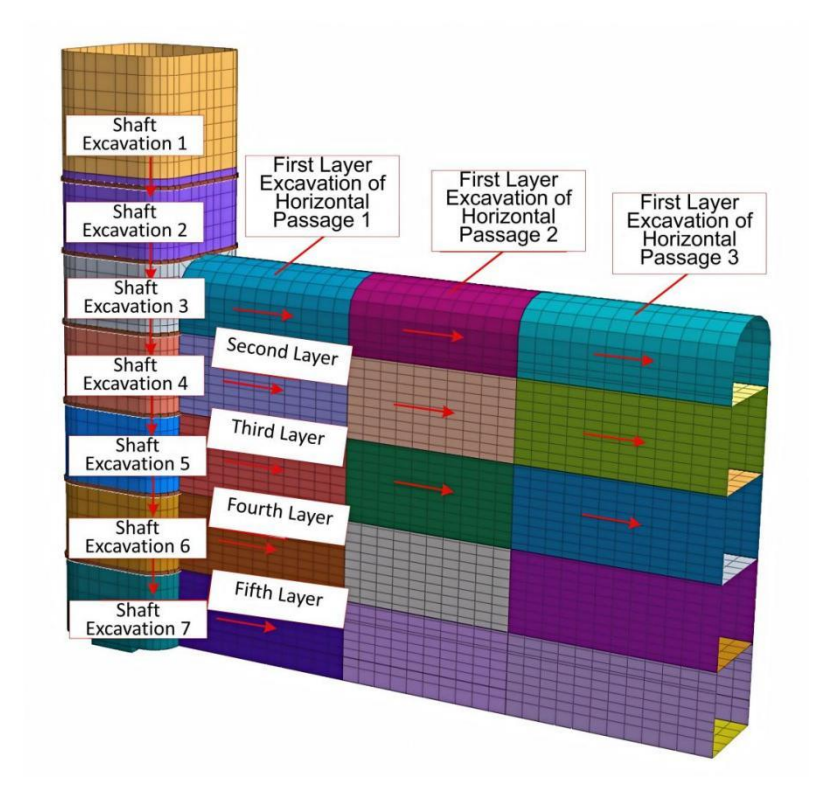


Fig. 5. Construction conditions setting for 1# shaft and cross passage excavation

The mechanical properties of the strata around the construction site play a crucial role in the force and deformation of the surrounding building complex during the construction of the No. 1 vertical shaft and the horizontal passage of the Memorial Hall Station. Therefore, when conducting three-dimensional simulation analysis and calculation, it is necessary to fully combine the distribution characteristics of the strata of this project and reasonably select the calculation parameters. The strata in the three-dimensional finite element calculation model are mainly simplified based on the engineering geological data near the No. 1 shaft and cross passage of the Memorial Hall station, mainly including plain fill soil, silty clay, fully weathered argillaceous siltstone, strongly weathered argillaceous siltstone, moderately weathered argillaceous siltstone, etc. The calculation parameters for each layer were determined mainly based on a comprehensive analysis of relevant engineering geological survey data and engineering experience; The mechanical calculation parameters of the No. 1 shaft and cross passage and the foundation structure of the surrounding building complex were determined based on the relevant design and construction drawings and after comprehensive consideration of relevant factors. The specific values of some models are shown in Tables 1-2. The boundary conditions of the three-dimensional finite element calculation model are: displacement

constraint at the bottom of the model in the Z direction, y-direction constraint at the front and back of the model, and X-direction constraint on the left and right sides of the model. The main process of the three-dimensional dynamic construction simulation of the impact of the No. 1 shaft and cross passage of the Memorial Hall Station on the foundation structure of the surrounding building complex is: initial stress field analysis, shaft excavation; Excavation of the cross passage, the conditions of this three-dimensional numerical simulation are shown in Table 3.

Table 1. 3D Numerical simulation material parameter values table

Materials	Constitutive model	Bulk density Gamma (kN/m³)	Cohesion <i>C(kPa)</i>	Internal friction Angle (φ)	Elastic modulus E(MPa)	Poisson's ratio (μ)
Plain fill soil	Mohr- Coulomb Model	19	17.	16	10	0.30
Silty clay	Mohr- Coulomb Model	18	19	19	15	0.35
Fully weathered argillaceous siltstone	Mohr- Coulomb Model	21	34	26	45	0.23
Strongly weathered argillaceous siltstone	Mohr- Coulomb Model	20	200	28	100	0.20
Moderately weathered argillaceous siltstone	Mohr- Coulomb Model	26	500	33	500	0.18
C25 concrete	Linear elasticity	25	-	-	28000	0.25
C30 concrete	Linear elasticity	25	-	-	30000	0.20
Steel	Wire elasticity	78	-	-	200000	0.30

Table 2. Three-dimensional numerical simulation unit parameter table

Unit Name	Material Properties	Unit attribute	Cell Size(mm)
Plain fill soil	Plain fill soil	Three-dimensional solid unit	-
Silty clay	Silty clay	Three-dimensional solid units	-
Fully weathered argillaceous siltstone	Fully weathered argillaceous siltstone	Three-dimensional solid unit	-
Strongly weathered argillaceous siltstone	Strongly weathered argillaceous siltstone	Three-dimensional solid unit	-
Weathered argillaceous siltstone	Moderately weathered argillaceous siltstone	Three-dimensional solid unit	-
Building shallow foundation	C30 concrete	Three-dimensional solid units	
Shotcrete support	C25 concrete	Plate unit	300mm
Shaft anchor bolts	Steel	Wire unit	Ф 40 mm
cross passage	Steel	Wire unit	Ф 20 mm
High-rise building piles	C30 concrete	Line unit	Ф 400 mm
Building columns	C30 concrete	Line unit	400*400mm

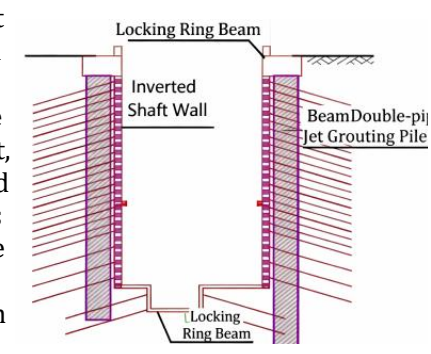
Table 3. Construction conditions

Construction conditions	Main construction contents
Working Condition 1	Analysis of the initial in-situ stress field of the site
Condition 2	Double-row micro-steel pipe pile reinforcement
Condition 3	Lock mouth ring beam and double-pipe jet grouting pile construction
Condition 4	Shaft excavation 1
Working Condition 5	Shaft excavation 2
Working Condition 6	Shaft excavation 3
Condition 7	cross passage advanced small conduit support construction
Condition 8	Excavation of the first level of the cross passage 1
Condition 9	Excavation of the first layer of the horizontal passage 2
Condition 10	Excavation of the first level of the cross passage 3
Condition 11	Shaft excavation 4
Working Condition 12	Excavation of the second layer of the cross passage 1
Condition 13	Second layer excavation of the cross passage 2
Condition 14	Second layer excavation of the cross passage 3
Condition 15	Shaft excavation 5
Condition 16	Excavation of the third level of the cross passage 1
Condition 17	Excavation of the third layer of the horizontal passage 2
Condition 18	Excavation of the third level of the cross passage 3
Condition 19	Shaft excavation 6
Working Condition 20	Excavation of the fourth level of the cross passage 1
Condition 21	Excavation of the fourth level of the cross passage 2
Condition 22	Excavation of the fourth level of the cross passage 3
Condition 23	Shaft excavation 7
Working Condition 24	Excavation of the fifth level of the cross passage 1
Condition 25	Excavation of the fifth floor of the horizontal passage 2
Condition 26	Excavation of the fifth floor of the cross passage 3
Construction conditions	Main construction contents
Working Condition 1	Analysis of the initial in-situ stress field of the site
Condition 2	Double-row micro-steel pipe pile reinforcement

Table 4. Construction sequence and staging

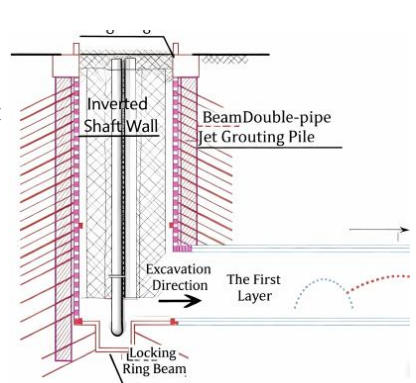
Serial Number	Process Description	Process Schedule Chart
1	①Pipeline relocation within the shaft range and construction of jet grouting piles. ②Construction of the shaft mouth locking ring beam; the next work can only be carried out when the strength of C30 concrete reaches more than 80%	Locking Ring Beam BeamDouble-pipe Jet Grouting Pile

- ①After the construction of the shaft mouth locking ring beam is completed, the construction of the inverted shaft wall will start below it, which adopts the support system of grid steel frame + shotcrete + grouted anchor pipe.
- ②When the shaft is constructed to a depth of 12.5m, the temporary bottom sealing of the shaft shall be carried out, and then the construction of the advanced large pipe shed in the pipe shed cave shall start. After the construction is completed, the shaft shall continue to be excavated to the elevation position of the temporary inverted arch of the first layer of the cross passage, and the secondary bottom sealing of the shaft shall be conducted.

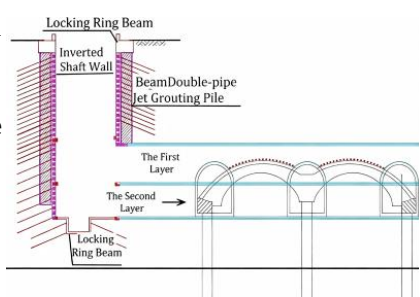


Key Terminology Explanati

- ①Attention shall be paid to pre-embedding the guide pipes for the large pipe shed above the shaft adit portal. When excavating to the adit portal, the large pipe shed shall be installed in one go at an upward horizontal angle of $1-3^{\circ}$.
- ②Before excavating the adit portal, a water detection test shall be conducted, and the water flow rate shall not exceed 0.1 L/min.
- ③The initial support and anchor pipes within the excavation contour of the first layer of the cross passage shall be chiseled off in sections, and four steel frames shall be installed consecutively at the adit portal.
 - ④After the excavation and support of the first layer of the cross passage are completed, construct the advanced support with small pipes for the small pilot tunnel, the large pipe shed at the arch crown of the station, and the advanced support with small pipes.



- ①After the excavation of the first layer of the cross passage is completed, the shaft shall continue to be excavated downward to the elevation of the temporary inverted arch of the second layer of the cross passage, and the temporary bottom sealing of the shaft shall be constructed.
- ②Chisel off the initial support and anchor rods within the excavation contour of the second layer of the cross passage in sections, and construct the second layer of the cross passage.
 - ③After the excavation and support of the second layer of the cross passage are completed, construct the small pilot tunnel, then carry out the construction of the side piles, middle columns, top longitudinal beams, initial support of the main arch and secondary lining of the station.



4.Results and Discussion

2

3

4

4.1Simulation Results and Analysis of The Impact of No. 1 Shaft and Cross Passage Construction at Memorial Hall Station on The Building Complex on The West Side

Fig.6 shows the zoning diagram and foundation number of the building complex on the west side, and Fig.7 shows the total displacement of the foundation structure of the building complex on the west side during the construction of the No. 1 shaft and the cross passage. Table 5 shows the summary of the displacement of the foundation structure of the building complex on the west side

under critical conditions during the construction of shaft 1 and passage, and Table 6 shows the calculation table of the maximum settlement difference of adjacent foundations of the building complex on the west side.

The three-dimensional simulation analysis of the impact of the construction process of No. 1 shaft and cross passage at Memorial Hall Station on the structure of the west building complex shows that the maximum horizontal X displacement induced by the construction process of No. 1 shaft and cross passage at Memorial Hall Station is 1.3mm, the horizontal Y displacement is 0.8mm, the maximum vertical displacement is 3.4mm, and the maximum total displacement is 3.7mm. The maximum settlement difference between adjacent foundations is 0.91mm.

In summary, the construction of the No. 1 shaft and cross passage at Memorial Hall Station has caused a certain amount of displacement in the shallow foundations of the building complex on the west side. Given that the displacement of the existing west building complex structure induced by the construction of No. 1 shaft and cross passage is controllable and far less than the allowable value of building foundation deformation stipulated in the "Code for Design of Building Foundation of Guangdong Province" (DBJ 15-31-2016), it is considered that the construction of No. 1 shaft and cross passage of Memorial Hall Station does not endanger the safety of the west building complex. Therefore, it is considered that the construction of No. 1 shaft and cross passage at Memorial Hall Station on Line 13 has a relatively small impact on the safety of the structure of the west building complex. It is recommended that the monitoring data of the structure of the west building complex be closely monitored during the construction process and information-based construction be carried out.

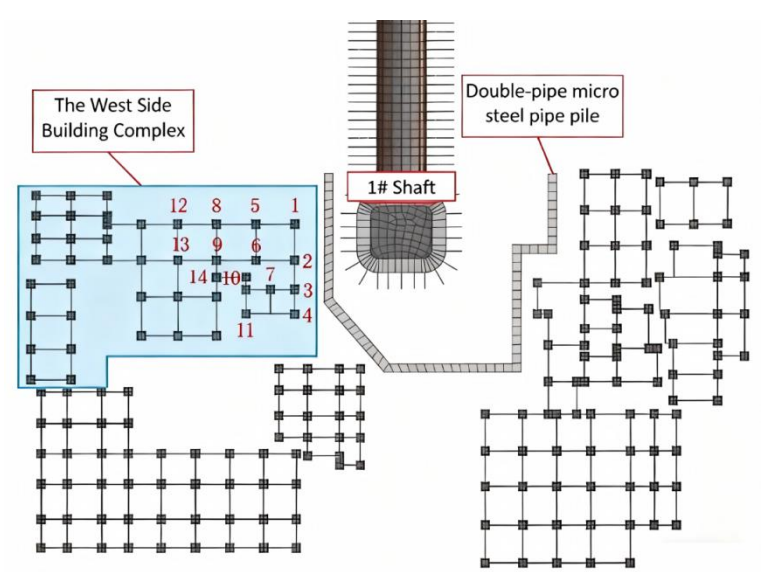


Fig. 6. Schematic diagram of the zoning and foundation number of the west building complex

Table 5. Summary Table of Foundation Displacement of the building complex on the West Side during the construction of No. 1 shaft and Cross Passage (mm)

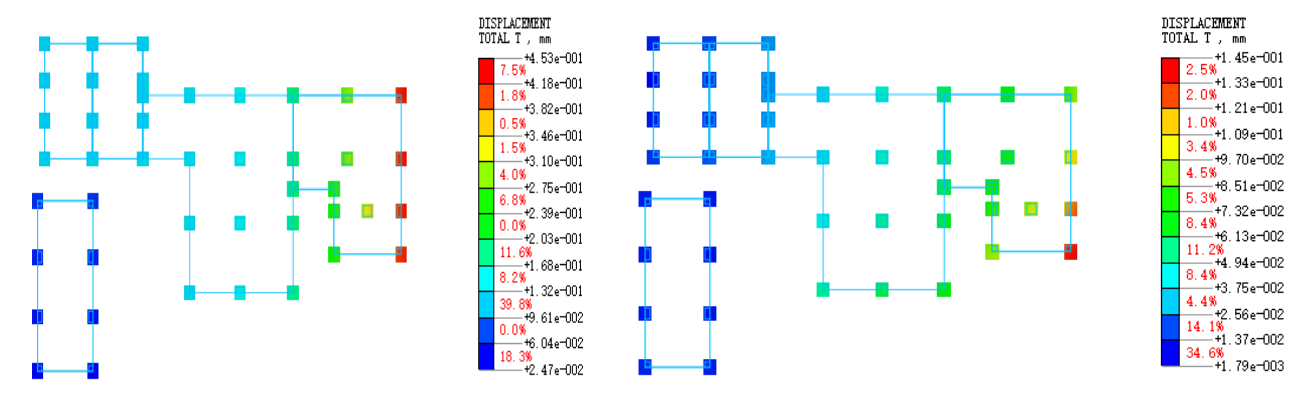
	Maximum displacement of the foundation(mm)					
Calculation of conditions	X-direction displacement	Y-direction displacement	Vertical displacement	Total displacement		
Analysis of the initial in-situ stress field of the site	0.0	0.0	0.0	0.0		
Double-row micro steel pipe pile reinforcement	0.1	0.1	0.4	0.5		
Lock mouth ring beam with double-pipe jet grouting pile construction	0.1	0.1	0.1	0.2		
Shaft excavation 1	0.3	0.2	0.9	0.9		

Shaft excavation 2	0.5	0.3	1.4	1.5
Shaft excavation 3	0.7	0.2	1.9	2.0
cross passage advanced small conduit support construction	0.6	0.3	1.8	1.9
Excavation of the first level of the cross passage 1	0.7	0.3	2.1	2.2
Excavation of the first level of the cross passage 2	0.8	0.4	2.2	2.3
Excavation of the first level of the cross passage 3	0.8	0.4	2.2	2.3
Shaft excavation 4	0.9	0.6	2.6	2.7
Second level excavation of the cross passage 1	1.0	0.6	2.8	3.0
Second level excavation of the cross passage 2	1.1	0.7	3.0	3.1
Second level excavation of the cross passage 3	1.2	0.7	3.0	3.2
Shaft excavation 5	1.2	0.8	3.2	3.4
Excavation of the third level of the cross passage 1	1.3	0.8	3.3	3.5
Excavation of the third level of the cross passage 2	1.3	0.9	3.4	3.6
Excavation of the third layer of the horizontal passage 3	1.3	0.8	3.4	3.7
Shaft excavation 6	1.3	0.8	3.4	3.6
Excavation of the fourth level of the cross passage 1	1.3	0.8	3.4	3.6
Excavation of the fourth level of the cross passage 2	1.3	0.8	3.4	3.6
Excavation of the fourth level of the cross passage 3	1.3	0.7	3.4	3.6
Shaft excavation 7	1.2	0.7	3.3	3.4
Excavation of the fifth level of the cross passage 1	1.2	0.6	3.2	3.4
Excavation of the fifth level of the cross passage 2	1.1	0.6	3.1	3.3
Excavation of the fifth level of the cross passage 3	1.1	0.7	3.1	3.2

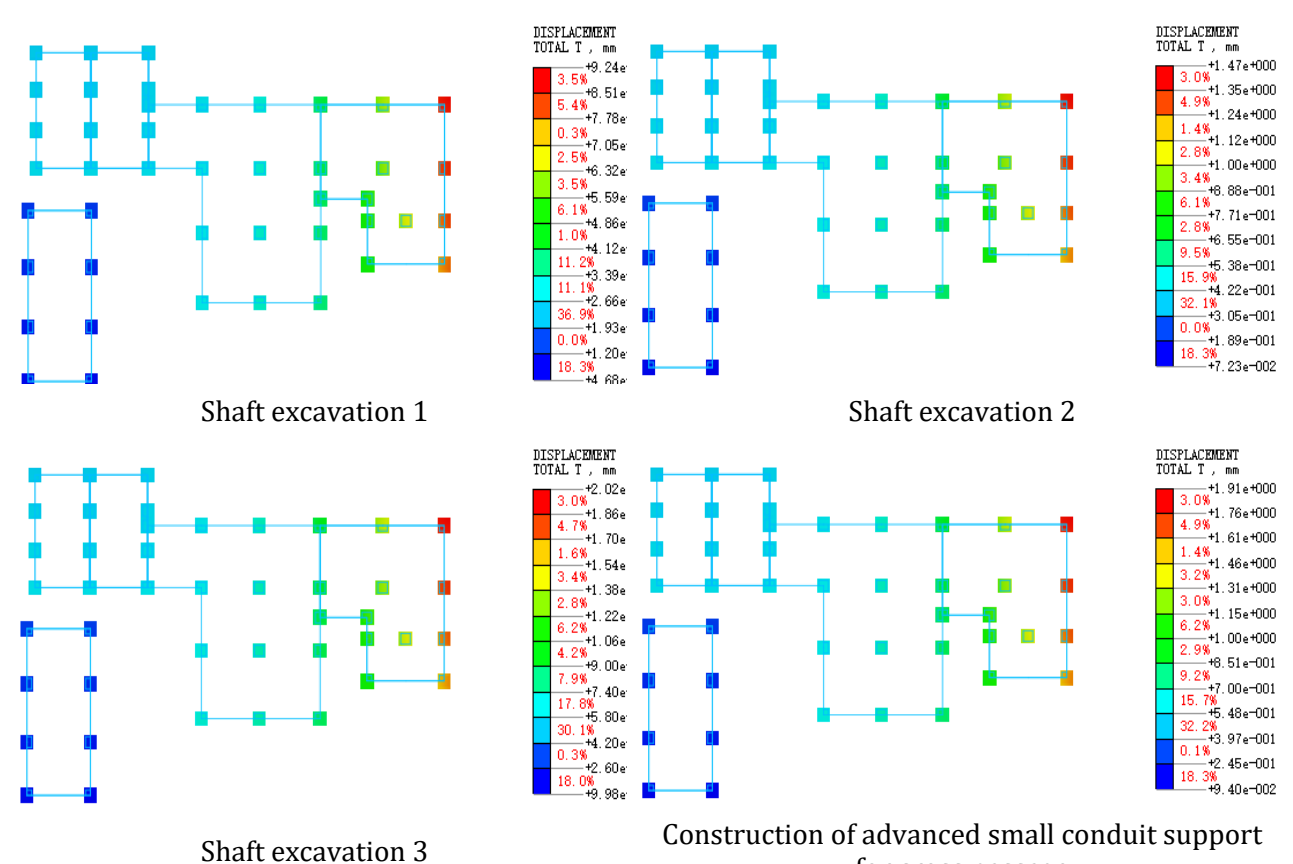
Table 6. Calculation table of maximum settlement difference between adjacent foundations of the west building complex (mm)

Adjacent pi	le numbers	Settlement difference (mm)	Pile spacing l (mm)	0.002 l
1	2	0.25	4000.00	8.00
2	3	0.21	4000.00	8.00
3	4	0.06	4000.00	8.00
1	5	0.91	4000.00	8.00
2	6	0.80	4000.00	8.00
3	7	0.49	4000.00	8.00
4	11	0.87	8000.00	16.00
5	6	0.19	4000.00	8.00

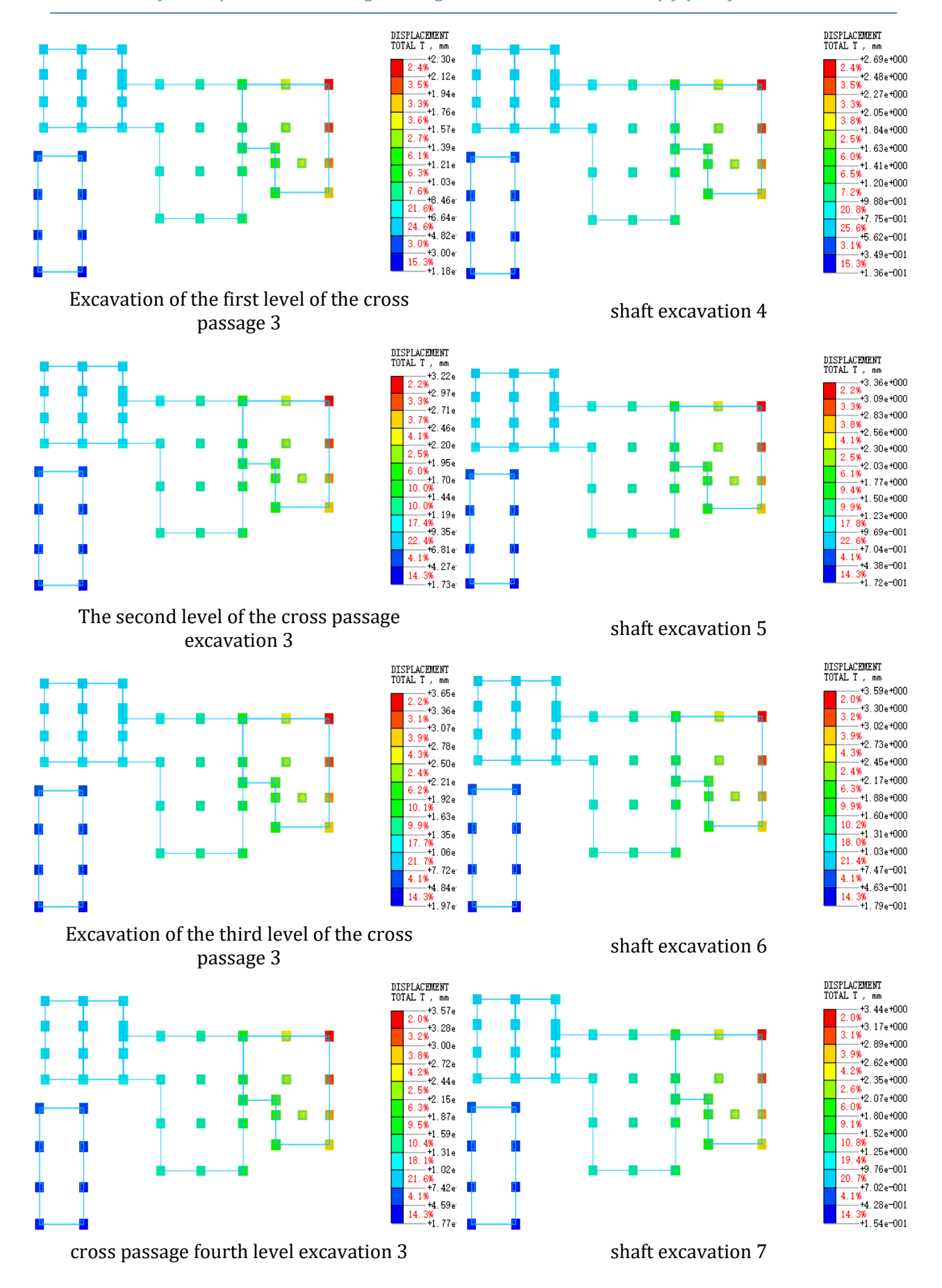
6	7	0.27	4000.00	8.00
7	11	0.17	4000.00	8.00
5	8	0.73	4000.00	8.00
6	9	0.71	4000.00	8.00
7	10	0.40	4500.00	9.00
8	9	0.10	4000.00	8.00
9	10	0.05	2000.00	4.00
8	12	0.45	4000.00	8.00
9	13	0.38	4000.00	8.00
10	14	0.52	4000.00	8.00
12	13	0.01	4000.00	8.00

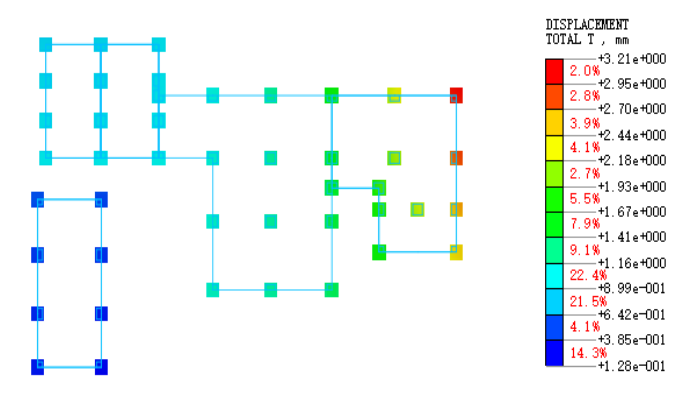


Double-row micro-steel pipe pile reinforced lock mouth ring beam with double-pipe jet grouting pile construction



for cross passage





Excavation of the fifth floor of the horizontal passage 3

Fig. 7. Total displacement of the foundation structure of the building complex on the west side (mm) under critical conditions during the construction of shaft No. 1 and cross passage

4.2Simulation Results and Analysis of The Impact of The Construction of No. 1 Shaft and Cross Passage at Memorial Hall Station on The Southwest Building (High-Rise)

Fig.8 shows the zoning diagram and foundation number of the building complex (high-rise) on the southwest side, and Fig.9 shows the total displacement of the foundation structure of the building complex (high-rise) on the southwest and west sides during the construction of the No. 1 shaft and cross passage. Table 7 shows the summary of pile foundation displacement of the southwest building complex (high-rise) under critical conditions during the construction of the No. 1 shaft and cross passage, and Table 8 shows the calculation table of the maximum settlement difference of adjacent foundations of the southwest building complex (high-rise).

The three-dimensional simulation analysis of the impact of the construction process of No. 1 shaft and cross passage at Memorial Hall Station on the structure of the southwest building complex (high-rise) shows that: The construction process of the No. 1 shaft and cross passage of the Memorial Hall Station induced the maximum horizontal X displacement of the pile foundation structure of the building complex (high-rise) on the southwest side to be 0.3mm, the horizontal Y displacement was 0.5mm, the maximum vertical displacement was 0.3mm, and the maximum total displacement was 0.6mm. The maximum settlement difference between adjacent foundations is 0.06mm.

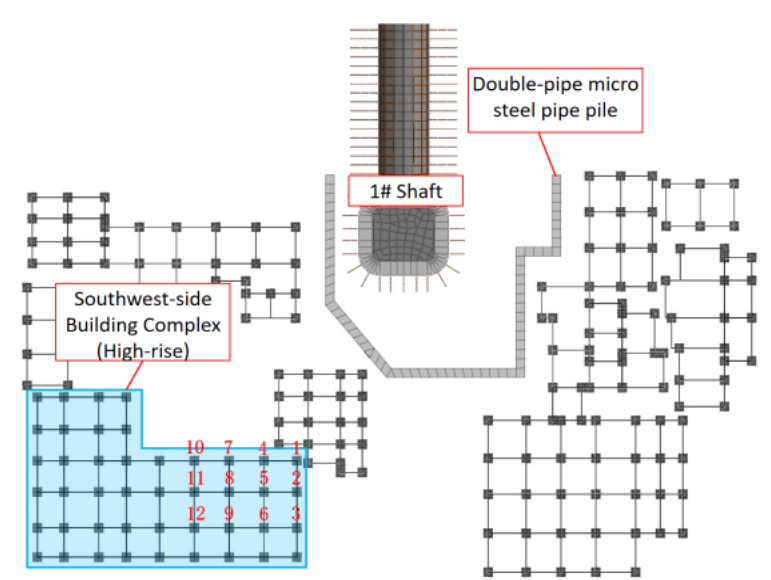


Fig. 8. Zoning diagram and foundation number of the southwest building complex (high-rise)

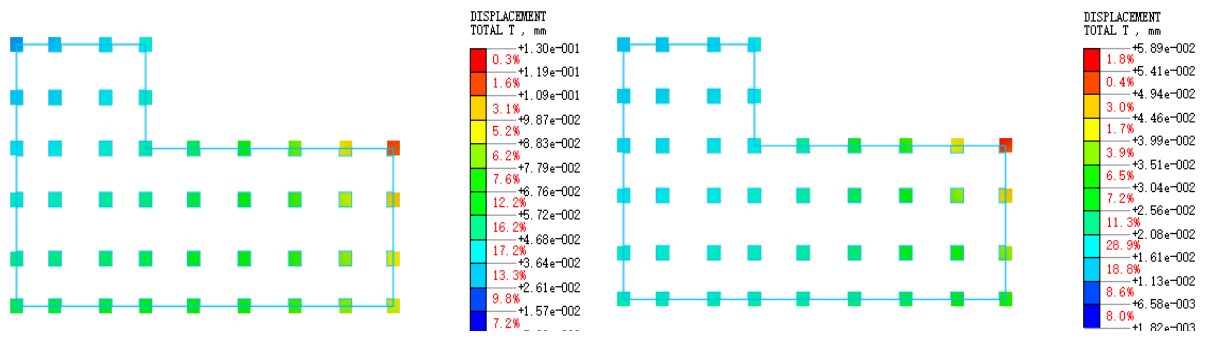
Table 7. Summary of Foundation Displacement of Buildings (high-rise) on the southwest and west sides during the construction of No. 1 shaft and Cross passage (mm)

	Maximum displacement of the foundation(mm)				
Calculation of conditions	X-direction displacement	Y-direction displacement	Vertical displacement	Total displacement	
Analysis of the initial in-situ stress field of the site	0.0	0.0	0.0	0.0	
Double-row micro-steel pipe pile reinforcement	0.1	0.1	0.1	0.1	
Construction of lock mouth ring beams and double-pipe jet grouting piles	0.1	0.1	0.1	0.1	
Shaft excavation 1	0.1	0.1	0.1	0.2	
Shaft excavation 2	0.1	0.2	0.2	0.3	
Shaft excavation 3	0.2	0.3	0.3	0.3	
cross passage advanced small conduit support construction	0.2	0.3	0.3	0.4	
Excavation of the first level of the cross passage 1	0.2	0.3	0.3	0.4	
Excavation of the first level of the cross passage 2	0.2	0.3	0.3	0.4	
Excavation of the first level of the cross passage 3	0.2	0.3	0.3	0.4	
Shaft excavation 4	0.2	0.4	0.3	0.5	
Second level excavation of the cross passage 1	0.2	0.4	0.3	0.6	
Second level excavation of the cross passage 2	0.2	0.5	0.3	0.6	
Second level excavation of the cross passage 3	0.2	0.5	0.3	0.6	
Shaft excavation 5	0.2	0.5	0.3	0.6	
Excavation of the third level of the cross passage 1	0.3	0.5	0.4	0.6	
Excavation of the third level of the cross passage 2	0.3	0.5	0.3	0.6	
Excavation of the third level of the cross passage 3	0.3	0.5	0.3	0.6	
Shaft excavation 6	0.2	0.5	0.3	0.6	
Excavation of the fourth level of the cross passage 1	0.2	0.5	0.3	0.6	
Excavation of the fourth level of the cross passage 2	0.2	0.5	0.3	0.6	
Excavation of the fourth level of the cross passage 3	0.2	0.5	0.3	0.6	
Shaft excavation 7	0.2	0.4	0.3	0.5	
Excavation of the fifth level of the cross passage 1	0.2	0.4	0.3	0.5	
Excavation of the fifth level of the cross passage 2	0.2	0.4	0.3	0.5	
Excavation of the fifth level of the cross passage 3	0.2	0.3	0.3	0.4	

In summary, the construction of the No. 1 shaft and cross passage at Memorial Hall Station has caused a certain displacement of the pile foundation of the building complex (high-rise) on the southwest side. Given that the displacement of the existing southwest building complex (high-rise) structure induced by the construction of No. 1 shaft and cross passage is controllable and far less than the allowable value of building foundation deformation stipulated in the "Code for Design of Building Foundation of Guangdong Province" (DBJ 15-31-2016), it is considered that the construction of No. 1 shaft and cross passage of Memorial Hall Station does not endanger the safety of the southwest building complex (high-rise). Therefore, it is considered that the construction of the No. 1 shaft and cross passage at the Memorial Hall Station of Line 13 has a relatively small impact on the safety of the building complex (high-rise) on the southwest side. It is recommended that the monitoring data of the building complex (high-rise) on the southwest side be closely monitored during the construction process and information-based construction be carried out.

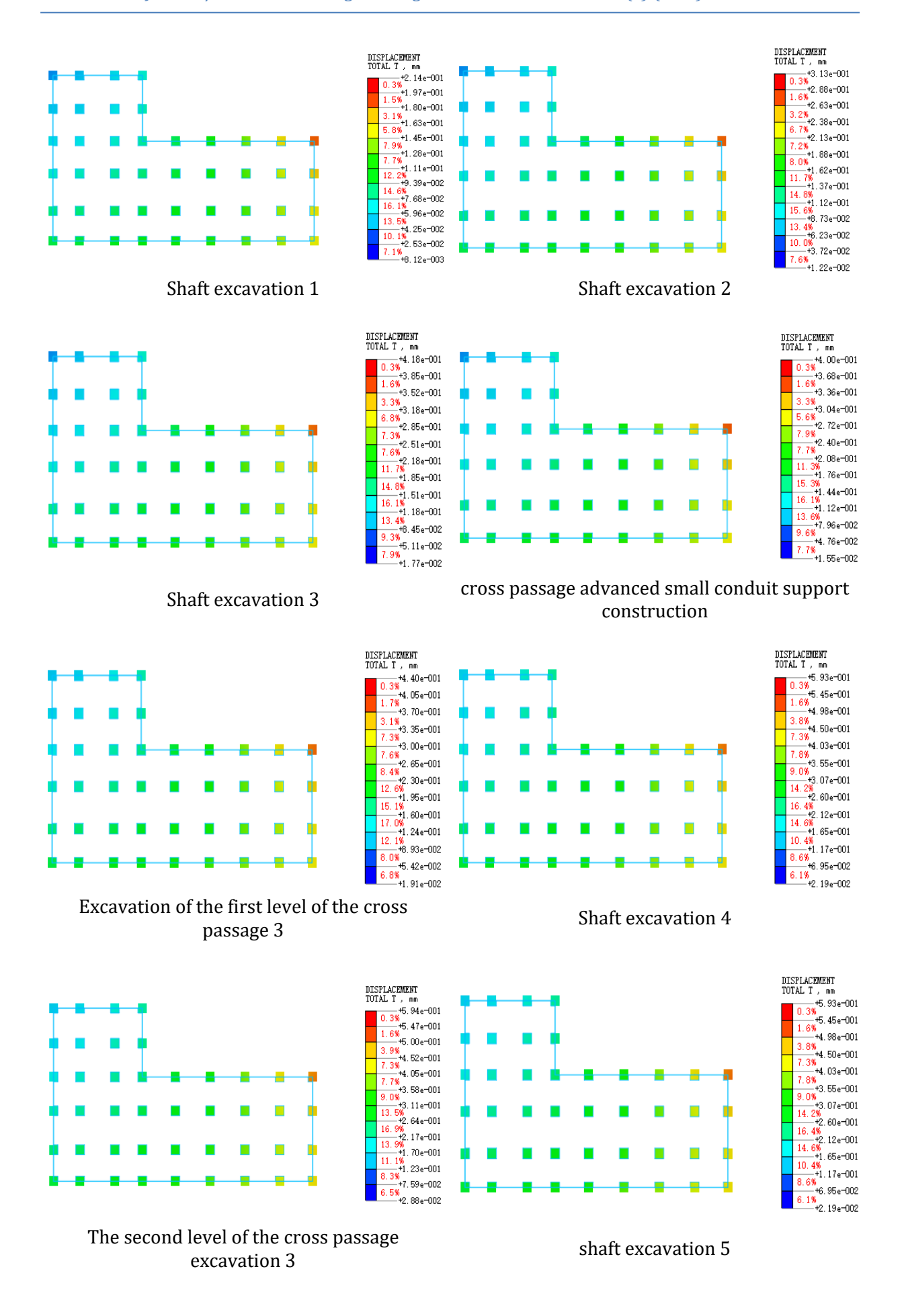
Table 8. Calculation table of maximum settlement difference between adjacent foundations of southwest building complex (high-rise) (mm)

Adjacent pi	ile numbers	Settlement difference (mm)	Pile spacing l (mm)	0.002 <i>l</i>
1	2	0.04	4000.00	8.00
2	3	0.02	4000.00	8.00
1	4	0.05	4000.00	8.00
2	5	0.04	4000.00	8.00
3	6	0.03	4000.00	8.00
4	5	0.03	4000.00	8.00
5	6	0.01	4000.00	8.00
4	7	0.06	4000.00	8.00
5	8	0.04	4000.00	8.00
6	9	0.03	4000.00	8.00
7	8	0.01	4000.00	8.00
8	9	0.01	4000.00	8.00
7	10	0.04	4000.00	8.00
8	11	0.03	4000.00	8.00
9	12	0.02	4000.00	8.00
10	11	0.01	4000.00	8.00
11	12	0.01	4000.00	8.00



Double-row micro steel pipe pile reinforcement

Lock mouth ring beam with double-pipe jet grouting pile construction



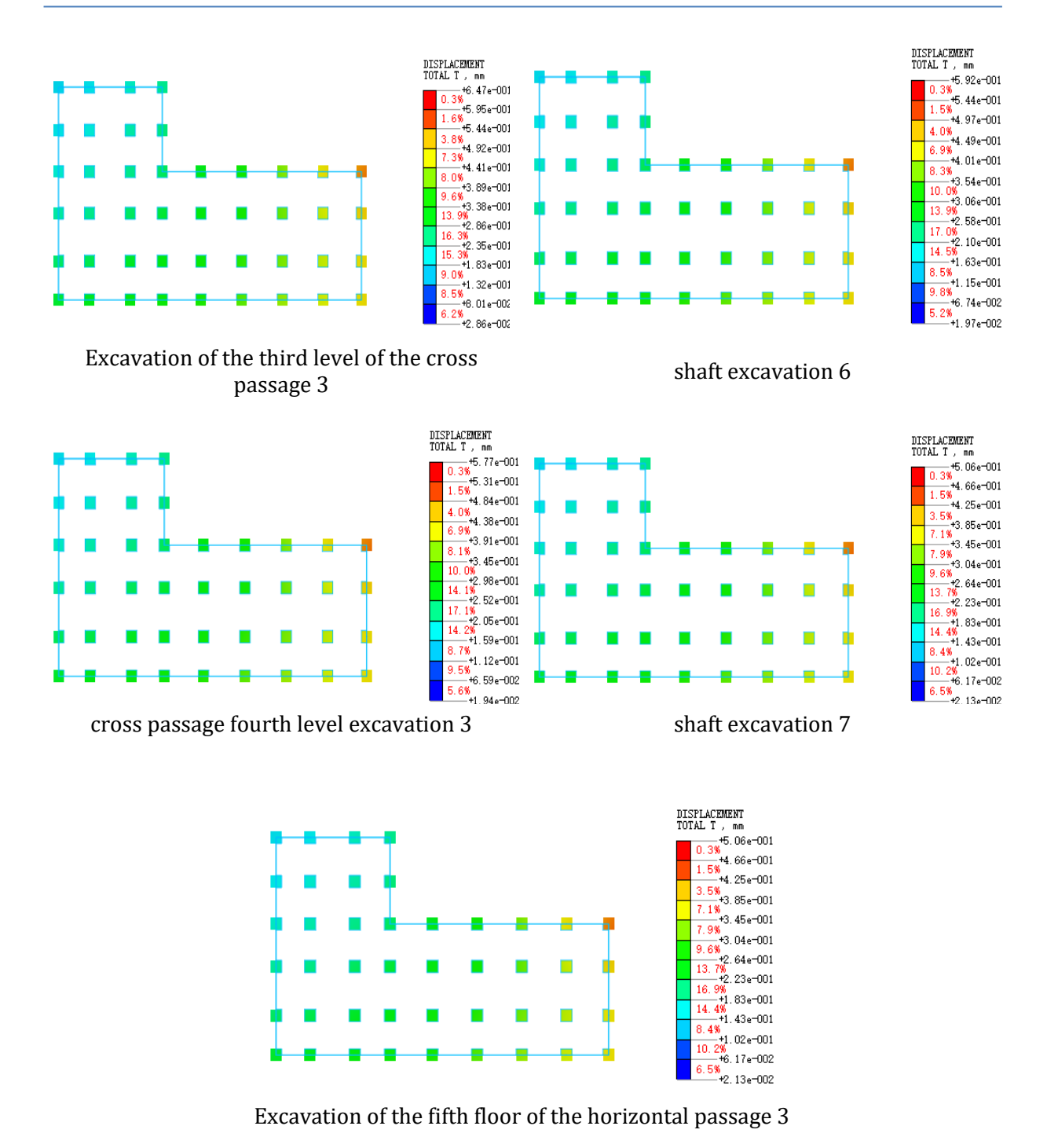


Fig. 9. Total displacement (mm) of foundation structure of high-rise building complex on the southwest side under key construction conditions of shaft no.1 and cross passage

4.3 Simulation Results and Analysis of the Impact of the Construction of Shaft No. 1 and Cross Passage at Memorial Hall Station on the East Side Building Complexes

Fig.10 presents the zoning diagram and foundation numbering of the eastern building complex, while Fig.11 shows the total displacement of the foundation structure of the eastern building complex during the construction of Shaft No. 1 and the cross passage. Table 9 is a summary table of the foundation structure displacement of the eastern building complex under key working conditions during the construction of Shaft No. 1 and the cross passage, and Table 10 is a calculation table for the settlement difference between adjacent foundations of the eastern building complex.

The displacement results from the 3D simulation analysis on the structural impact of the eastern building complex during the construction of Shaft No. 1 and the cross passage at Jiniantang Station

indicate that: during the construction of Shaft No. 1 and the cross passage at Jiniantang Station, the maximum horizontal X-displacement, horizontal Y-displacement, maximum vertical displacement, and maximum total displacement of the shallow foundation structure of the eastern building complex induced by the construction are 1.3 mm, 0.7 mm, 2.2 mm, and 2.4 mm respectively. The maximum settlement difference between adjacent foundations is 0.60 mm.

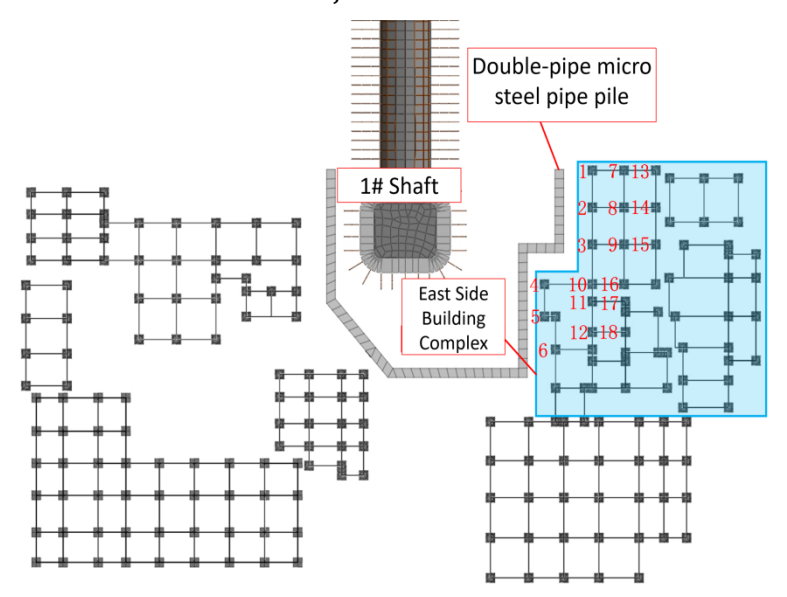


Fig. 10. Schematic diagram of zoning and foundation numbering for the east side building complex

Table 9. Summary table of foundation structure displacements of the east side building complex during the construction of shaft no. 1 and cross passages (mm)

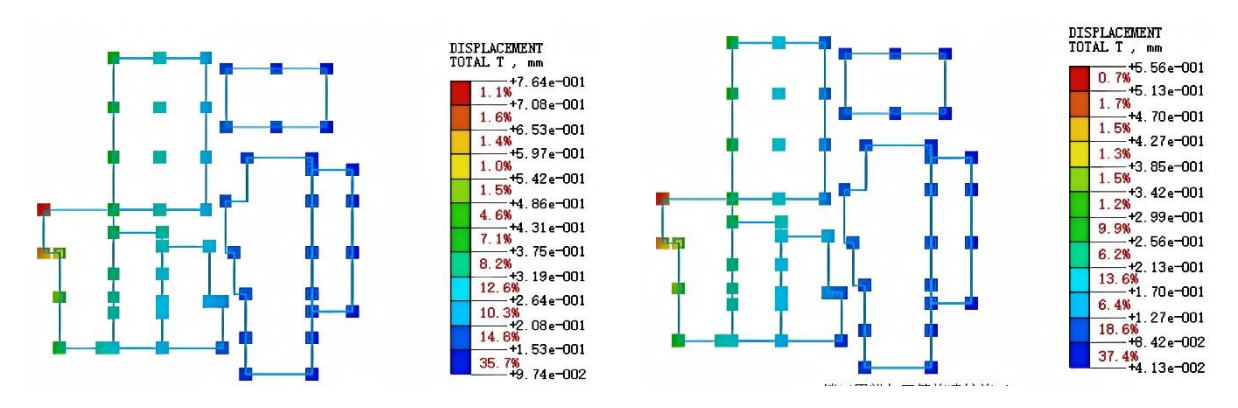
	Maximum displacement of the foundation(mm)				
Calculation of conditions	X-direction displacement	Y-direction displacement	Vertical displacement	Total displacement	
Analysis of the initial in-situ stress field of the site	0.0	0.0	0.0	0.0	
Double-row micro-steel pipe pile reinforcement	0.2	0.1	0.7	0.8	
Lock mouth ring beam with double-pipe iet grouting pile construction	0.1	0.1	0.7	0.6	
Shaft excavation 1	0.3	0.1	1.0	1.0	
Shaft excavation 2	0.5	0.2	1.2	1.3	
Shaft excavation 3	0.6	0.3	1.5	1.6	
cross passage advanced small conduit	0.6	0.3	1.5	1.6	
Excavation of the first level of the cross passage 1	0.7	0.4	1.6	1.7	
Excavation of the first level of the cross	0.7	0.4	1.6	1.7	
Excavation of the first level of the cross passage 3	0.8	0.4	1.6	1.7	
Shaft excavation 4	0.9	0.5	1.8	2.0	
Second level excavation of the cross passage 1	1.0	0.6	2.0	2.1	
Second level excavation of the cross	1.1	0.6	2.0	2.2	
Second level excavation of the cross passage 3	1.2	0.6	2.0	2.2	

Shaft excavation 5	1.2	0.6	2.1	2.3
Excavation of the third layer of the horizontal passage 1	1.3	0.7	2.2	2.4
Excavation of the third level of the cross passage 2	1.3	0.7	2.2	2.4
Excavation of the third level of the cross passage 3	1.3	0.7	2.2	2.4
Shaft excavation 6	1.3	0.7	2.2	2.4
Excavation of the fourth level of the cross passage 1	1.3	0.7	2.2	2.4
Excavation of the fourth level of the cross passage 2	1.3	0.7	2.2	2.4
Excavation of the fourth level of the cross passage 3	1.3	0.7	2.2	2.4
Shaft excavation 7	1.3	0.6	2.1	2.3
Excavation of the fifth level of the cross passage 1	1.2	0.6	2.1	2.3
Excavation of the fifth level of the cross	1.2	0.6	2.0	2.2
bassage 2 Excavation of the fifth level of the cross passage 3	1.2	0.6	2.0	2.2

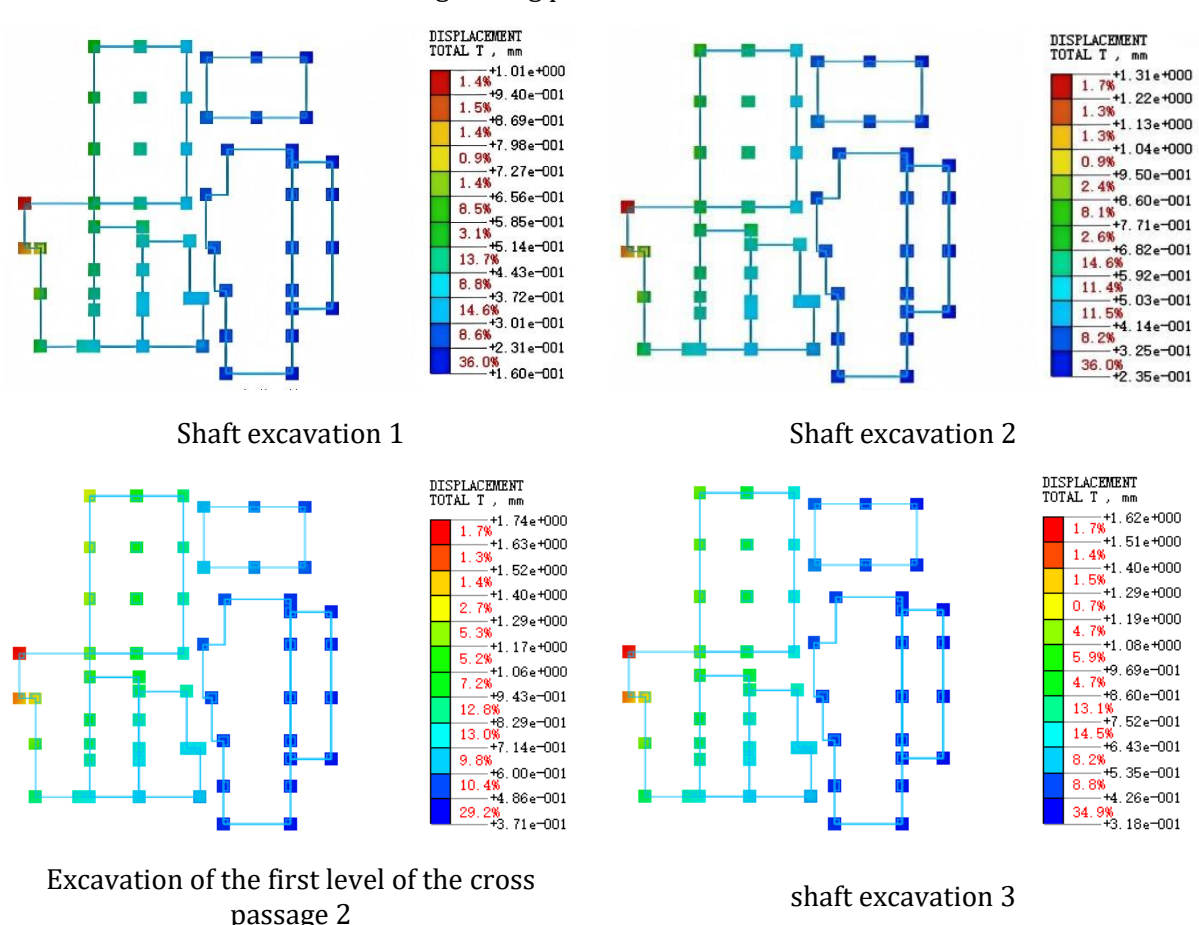
Table 10. Calculation table of maximum settlement difference between adjacent foundations of the east side building complex (mm)

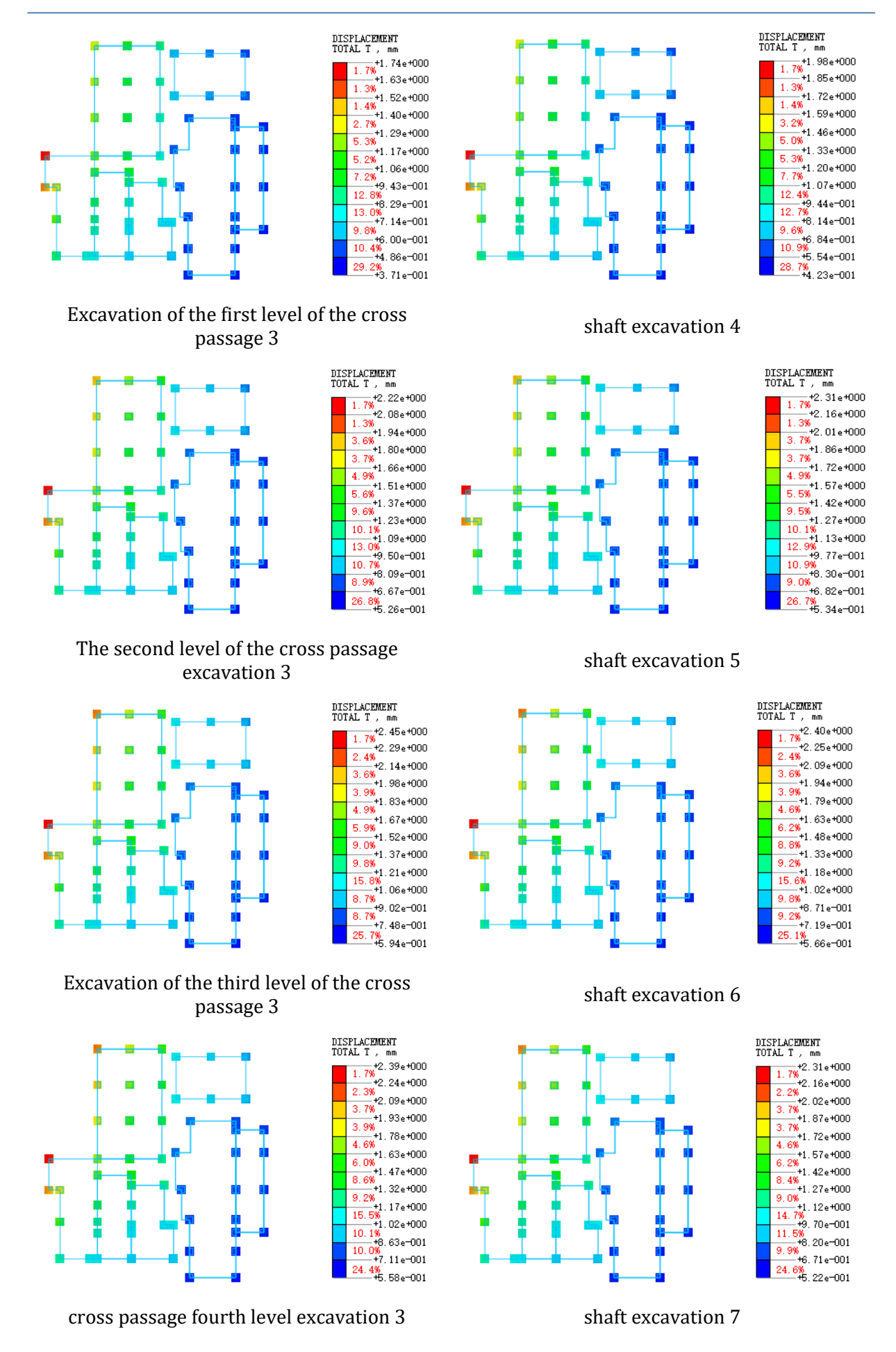
Adjacent p	ile numbers	Settlement difference (mm)	Pile spacing l (mm)	0.002 l
1	2	0.11	4000.00	8.00
2	3	0.10	4000.00	8.00
3	4	0.42	9000.00	18.0
4	5	0.17	4000.00	8.00
5	6	0.45	4000.00	8.00
1	7	0.29	4000.00	8.00
2	8	0.28	4000.00	8.00
3	9	0.28	4000.00	8.00
4	10	0.60	5000.00	10.0
5	11	0.48	5500.00	11.0
6	12	0.18	4500.00	9.00
7	8	0.10	4000.00	8.00
8	9	0.10	4000.00	8.00
9	10	0.15	6000.00	12.0
10	11	0.09	2000.00	4.00
11	12	0.20	4000.00	8.00
7	13	0.30	4000.00	8.00
8	14	0.22	4000.00	8.00
9	15	0.23	4000.00	8.00
10	16	0.21	4000.00	8.00
11	17	0.21	4000.00	8.00
12	18	0.16	4000.00	8.00
13	14	0.10	4000.00	8.00
14	15	0.10	4000.00	8.00
15	16	0.09	6000.00	12.0
16	17	0.02	4000.00	8.00
17	18	0.17	4000.00	8.00

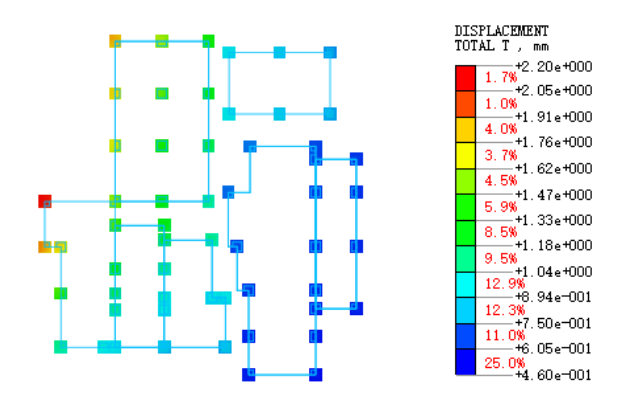
In conclusion, the construction of Shaft No. 1 and the cross passage at Jiniantang Station has induced a certain amount of displacement in the shallow foundations of the eastern building complex. Given that the displacement of the existing eastern building complex structure induced by the construction of Shaft No. 1 and the cross passage is controllable and far smaller than the allowable value for building foundation deformation specified in Guangdong Provincial Code for Design of Building Foundation (DBJ 15-31-2016), it is considered that the construction of Shaft No. 1 and the cross passage at Jiniantang Station does not endanger the safety of the eastern building complex. Therefore, it is concluded that the construction of Shaft No. 1 and the cross passage at Jiniantang Station of Line 13 has a relatively small impact on the structural safety of the eastern building complex. It is recommended to closely monitor the monitoring data of the eastern building complex structure during the construction process and implement information-based construction.



Double-row micro steel pipe pile reinforcement of lock mouth ring beam and double-pipe jet grouting pile construction







Excavation of the fifth level of the cross passage 3

Fig. 11. Total displacement of foundation structures of the east side building complex under key working conditions during the construction of shaft no. 1 and cross passages (mm)

4.4 Simulation Results and Analysis of The Impact of The Construction of No. 1 Shaft and Cross Passage at Memorial Hall Station on The Southwest Building (Bungalow)

Fig.12 shows the zoning diagram and foundation number of the building complex (bungalow) on the southwest side, and Fig.13 shows the total displacement of the foundation structure of the building complex (bungalow) on the southwest and west sides during the construction of the No. 1 shaft and cross passage. Table 11 shows the summary of the displacement of the shallow foundation structure of the southwest building complex (bungalow) under critical conditions during the construction of the No. 1 shaft and the cross passage, and Table 12 shows the calculation table of the maximum settlement difference of adjacent foundations of the southwest building complex (bungalow).

The three-dimensional simulation analysis of the impact of the construction process of No. 1 shaft and cross passage at Memorial Hall Station on the structure of the southwest building complex (bungalow) shows that: The construction process of the No. 1 shaft and cross passage of the Memorial Hall Station induced the maximum horizontal X displacement of the shallow foundation structure of the southwest building complex (bungalow) to be 0.4mm, the horizontal Y displacement to be 1.0mm, the maximum vertical displacement to be 2.2mm, and the maximum total displacement to be 2.5mm. The maximum settlement difference between adjacent foundations is 0.32mm.

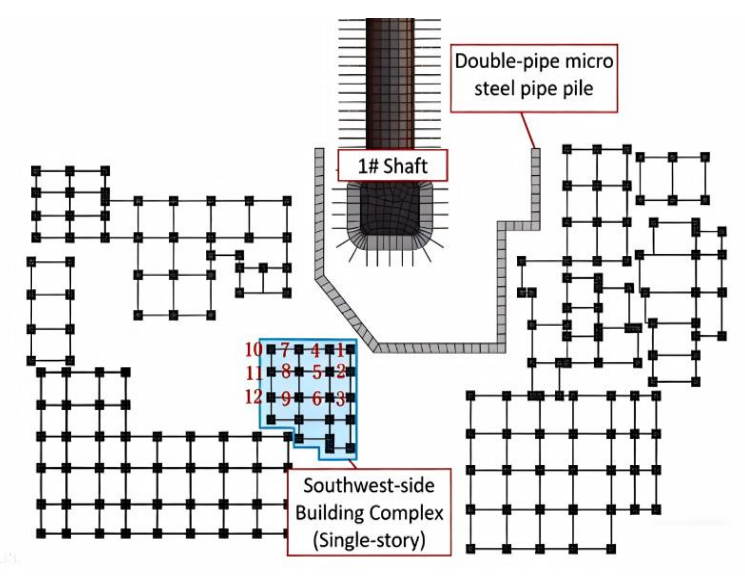


Fig. 12. Zoning diagram and foundation number of the southwest building complex (bungalows)

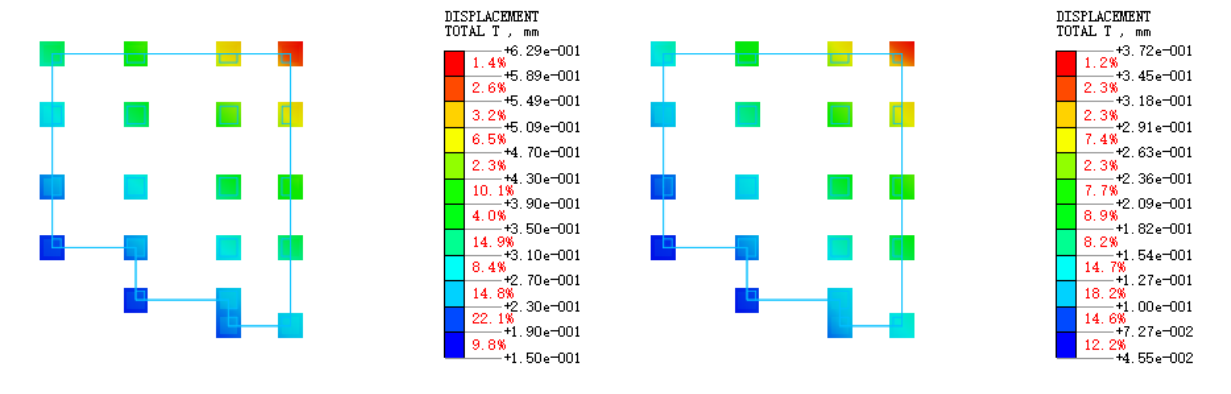
Table 11. Summary table of foundation displacement of buildings (bungalows) on the southwest and west sides during the construction of no. 1 shaft and cross passage (mm)

	Maximum displacement of the foundation(mm)						
Calculation of conditions	X-direction displacement	Y-direction displacement	Vertical displacement	Total displacement			
Analysis of the initial in-situ stress field of the site	0.0	0.0	0.0	0.0			
Double-row micro-steel pipe pile reinforcement	0.1	0.1	0.6	0.6			
Lock mouth ring beam with double- pipe jet grouting pile construction	0.1	0.1	0.4	0.4			
Shaft excavation 1	0.2	0.3	0.9	0.9			
Shaft excavation 2	0.2	0.4	1.2	1.3			
Shaft excavation 3	0.3	0.6	1.6	1.7			
cross passage advanced small conduit support construction	0.3	0.5	1.5	1.6			
Excavation of the first level of the cross passage 1	0.3	0.6	1.6	1.8			
Excavation of the first level of the cross passage 2	0.3	0.6	1.6	1.8			
Excavation of the first level of the cross passage 3	0.3	0.6	1.6	1.8			
Shaft excavation 4	0.3	0.7	1.9	2.1			
Second level excavation of the cross passage 1	0.4	0.9	2.0	2.2			
Second level excavation of the cross passage 2	0.4	0.9	2.0	2.2			
Second level excavation of the cross passage 3	0.4	0.9	2.0	2.3			
Shaft excavation 5	0.4	0.9	2.1	2.3			
Excavation of the third layer of the horizontal passage 1	0.4	1.0	2.2	2.4			
Excavation of the third level of the cross passage 2	0.4	1.0	2.2	2.4			
Excavation of the third level of the cross passage 3	0.4	1.0	2.2	2.5			
Shaft excavation 6	0.4	1.0	2.2	2.4			
Excavation of the fourth level of the cross passage 1	0.4	1.0	2.2	2.4			
Excavation of the fourth level of the cross passage 2	0.4	1.0	2.2	2.4			
Excavation of the fourth level of the cross passage 3	0.4	1.0	2.2	2.4			
Shaft excavation 7	0.4	0.9	2.1	2.3			
Excavation of the fifth level of the cross passage 1	0.4	0.9	2.0	2.2			
Excavation of the fifth level of the cross passage 2	0.4	0.8	2.0	2.1			
Excavation of the fifth level of the cross passage 3	0.4	0.8	2.0	2.1			

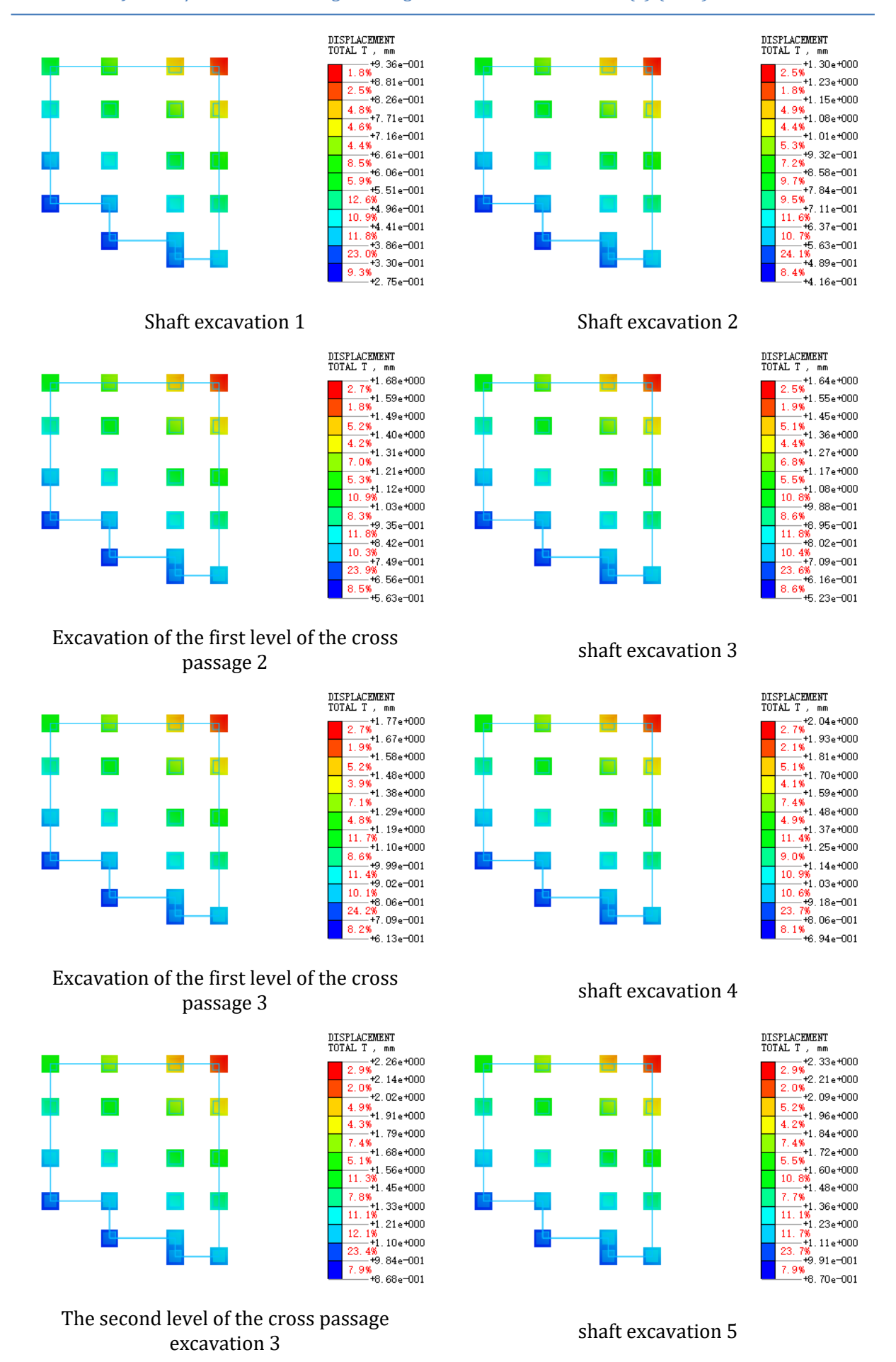
In summary, the construction of No. 1 shaft and cross passage at Memorial Hall Station has caused a certain amount of displacement in the shallow foundations of the building complex (bungalows) on the southwest side. Given that the displacement of the existing southwest building complex (bungalow) structure induced by the construction of No. 1 shaft and cross passage is controllable and far less than the allowable value of building foundation deformation in the "Code for Design of Building Foundation of Guangdong Province" (DBJ 15-31-2016), it is considered that the construction of No. 1 shaft and cross passage of Memorial Hall Station does not endanger the safety of the southwest building complex (bungalow). Therefore, it is considered that the construction of No. 1 shaft and cross passage at Memorial Hall Station on Line 13 has a relatively small impact on the structural safety of the building complex (bungalow) on the southwest side. It is recommended that the monitoring data of the building complex (bungalow) structure on the southwest side be closely monitored during the construction process and information-based construction be carried out.

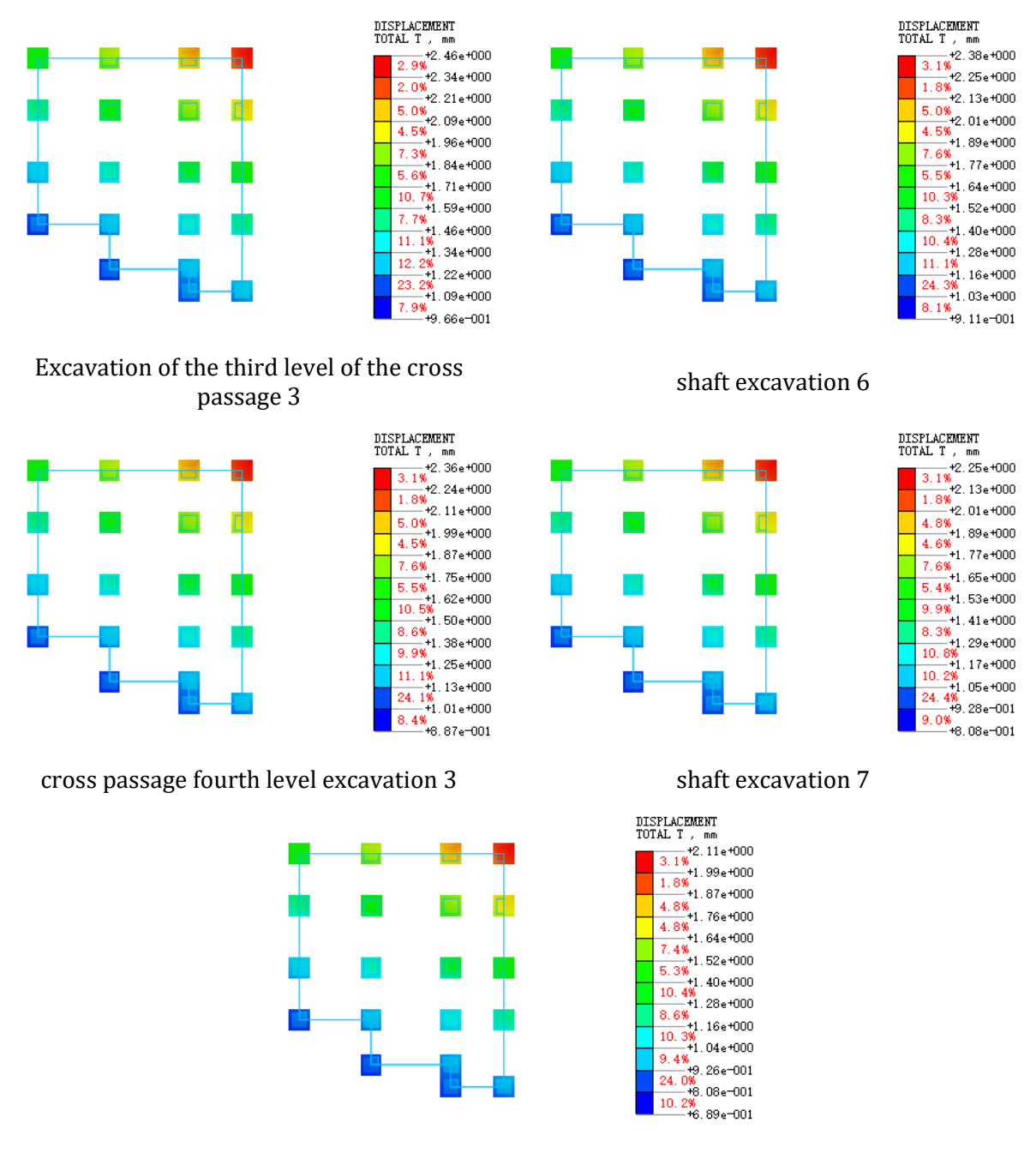
Table 12. Calculation table of maximum settlement difference between adjacent foundations of southwest building complex (bungalow) (mm)

Adjacent pi	nt pile numbers Settlement difference (mm)		Pile spacing l (mm)	0.002 l
1	2	0.30	4000.00	8.00
2	3	0.32	4000.00	8.00
1	4	0.14	4000.00	8.00
2	5	0.25	4000.00	8.00
3	6	0.12	4000.00	8.00
4	5	0.27	4000.00	8.00
5	6	0.31	4000.00	8.00
4	7	0.24	4000.00	8.00
5	8	0.22	4000.00	8.00
6	9	0.17	4000.00	8.00
7	8	0.25	4000.00	8.00
8	9	0.25	4000.00	8.00
7	10	0.19	4000.00	8.00
8	11	0.16	4000.00	8.00
9	12	0.13	4000.00	8.00
10	11	0.22	4000.00	8.00
11	12	0.21	4000.00	8.00



Double-row micro steel pipe pile reinforcement of lock mouth ring beam and double-pipe jet grouting pile construction





Excavation of the fifth level of the cross passage 3

Fig. 13. Critical conditions for the construction of 1# shaft and cross passage Total displacement of the foundation structure of the southwest building complex (bungalow) (mm)

4.5 Simulation Results and Analysis of the Impact of the Construction of Shaft No. 1 and cross passages at Jiniantang Station on the Southeast Building Complex

Fig.14 is the schematic diagram of zoning and numbering for the southeast building complex, while Fig.15 shows the total displacement of the foundation structure of the southeast building complex during the construction of Shaft No. 1 and the cross passages. Table 13 is a summary table of the foundation structure displacement of the southeast building complex under key working conditions during the construction of Shaft No. 1 and the cross passages, and Table 14 is a calculation table of the settlement difference between adjacent foundations of the southeast building complex.

The displacement results from the 3D simulation analysis on the structural impact of the construction of Shaft No. 1 and the cross passages at Jiniantang Station on the southeast building

complex indicate that: during the construction of Shaft No. 1 and the cross passages at Jiniantang Station, the maximum horizontal X-displacement, horizontal Y-displacement, maximum vertical displacement, and maximum total displacement of the shallow foundation structure of the southeast building complex induced by the construction are 0.6 mm, 0.6 mm, 1.1 mm, and 1.2 mm respectively. The maximum settlement difference between adjacent foundations is 0.22 mm.

In conclusion, the construction of Shaft No. 1 and the cross passages at Jiniantang Station has induced a certain amount of displacement in the shallow foundations of the southeast building complex. Given that the displacement of the existing structure of the southeast building complex induced by the construction of Shaft No. 1 and the cross passages is controllable and far smaller than the allowable value for building foundation deformation specified in Guangdong Provincial Code for Design of Building Foundations (DBJ 15-31-2016), it is considered that the construction of Shaft No. 1 and the cross passages at Jiniantang Station does not endanger the safety of the southeast building complex. Therefore, it is believed that the construction of Shaft No. 1 and the cross passages at Jiniantang Station of Line 13 has a minor impact on the structural safety of the southeast building complex. It is recommended to closely monitor the monitoring data of the structure of the southeast building complex during the construction process and carry out information-based construction.

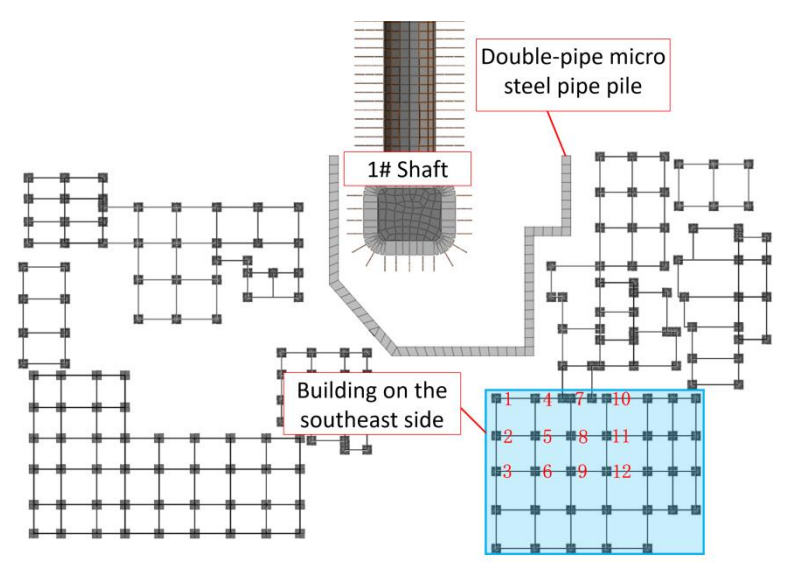


Fig 14. Zoning plan and foundation numbering of the building complex on the southeast side

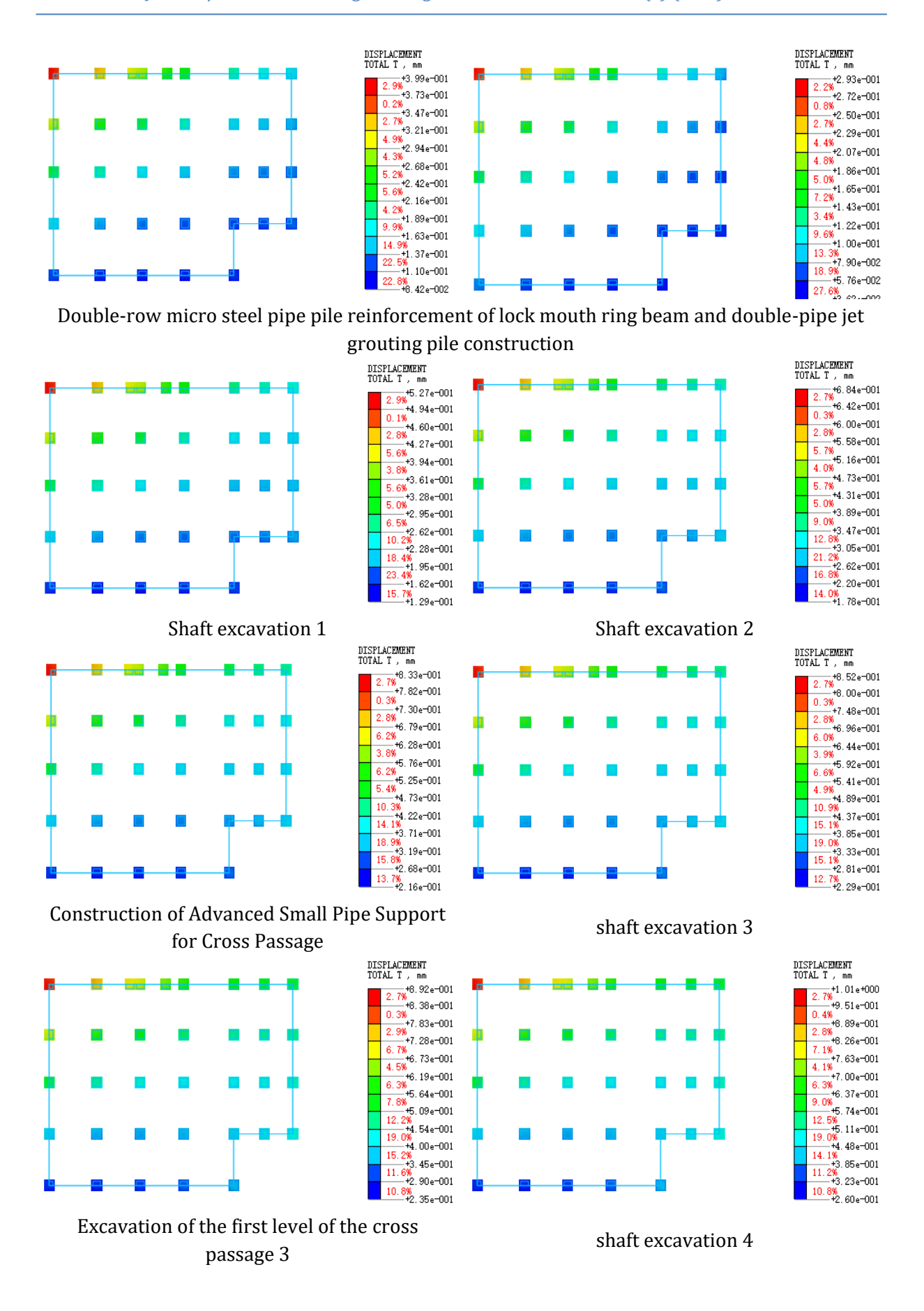
Table 13. Summary table of foundation structure displacements (mm) of the southeast building complex during the construction of shaft no.1 and cross passage

	Maximum displacement of the foundation(mm)						
Calculation of conditions	X-direction displacement	Y-direction displacement	Vertical displacement	Total displacement			
Analysis of the initial in-situ stress field of the site	0.0	0.0	0.0	0.0			
Double-row micro-steel pipe pile reinforcement	0.1	0.1	0.4	0.4			
Lock mouth ring beam with double- pipe jet grouting pile construction	0.1	0.1	0.3	0.3			
Shaft excavation 1	0.2	0.1	0.5	0.5			
Shaft excavation 2	0.3	0.2	0.6	0.7			
Shaft excavation 3	0.3	0.3	0.8	0.8			
cross passage advanced small conduit support construction	0.3	0.3	0.8	0.8			

Excavation of the first level of the cross passage 1	0.4	0.3	0.8	0.9
Excavation of the first level of the cross passage 2	0.4	0.3	0.8	0.9
Excavation of the first level of the cross passage 3	0.4	0.3	8.0	0.9
Shaft excavation 4	0.4	0.4	0.9	1.0
Second level excavation of the cross passage 1	0.5	0.4	1.0	1.1
Second level excavation of the cross passage 2	0.5	0.5	1.0	1.1
Second level excavation of the cross passage 3	0.5	0.5	1.0	1.1
Shaft excavation 5	0.5	0.5	1.0	1.1
Excavation of the third layer of the horizontal passage 1 Excavation of the third level of the	0.5	0.5	1.1	1.2
cross passage 2	0.5	0.5	1.1	1.2
Excavation of the third level of the cross passage 3	0.6	0.6	1.1	1.2
Shaft excavation 6	0.5	0.5	1.0	1.2
Excavation of the fourth level of the cross passage 1	0.5	0.5	1.0	1.2
Excavation of the fourth level of the cross passage 2	0.5	0.5	1.0	1.2
Excavation of the fourth level of the cross passage 3	0.5	0.5	1.0	1.1
Shaft excavation 7	0.5	0.5	1.0	1.1
Excavation of the fifth level of the cross passage 1	0.5	0.5	1.0	1.1
Excavation of the fifth level of the cross passage 2	0.5	0.5	0.9	1.0
Excavation of the fifth level of the cross passage 3	0.5	0.4	0.9	1.0

 $Table\ 14.\ Calculation\ Table\ of\ Maximum\ Settlement\ Difference\ of\ Adjacent\ Foundations\ in\ the\ Southeast\ Building\ Complex\ (mm)$

Adjacent pi	t pile numbers Settlement difference (mm)		Pile spacing l (mm)	0.0021
1	2	0.14	4000.00	8.00
2	3	0.22	4000.00	8.00
1	4	0.11	4000.00	8.00
2	5	0.09	4000.00	8.00
3	6	0.06	4000.00	8.00
4	5	0.22	4000.00	8.00
5	6	0.19	4000.00	8.00
4	7	0.08	4000.00	8.00
5	8	0.07	4000.00	8.00
6	9	0.03	4000.00	8.00
7	8	0.21	4000.00	8.00
8	9	0.15	4000.00	8.00
7	10	0.07	4000.00	8.00
8	11	0.04	4000.00	8.00
9	12	0.01	4000.00	8.00
10	11	0.18	4000.00	8.00
11	12	0.11	4000.00	8.00



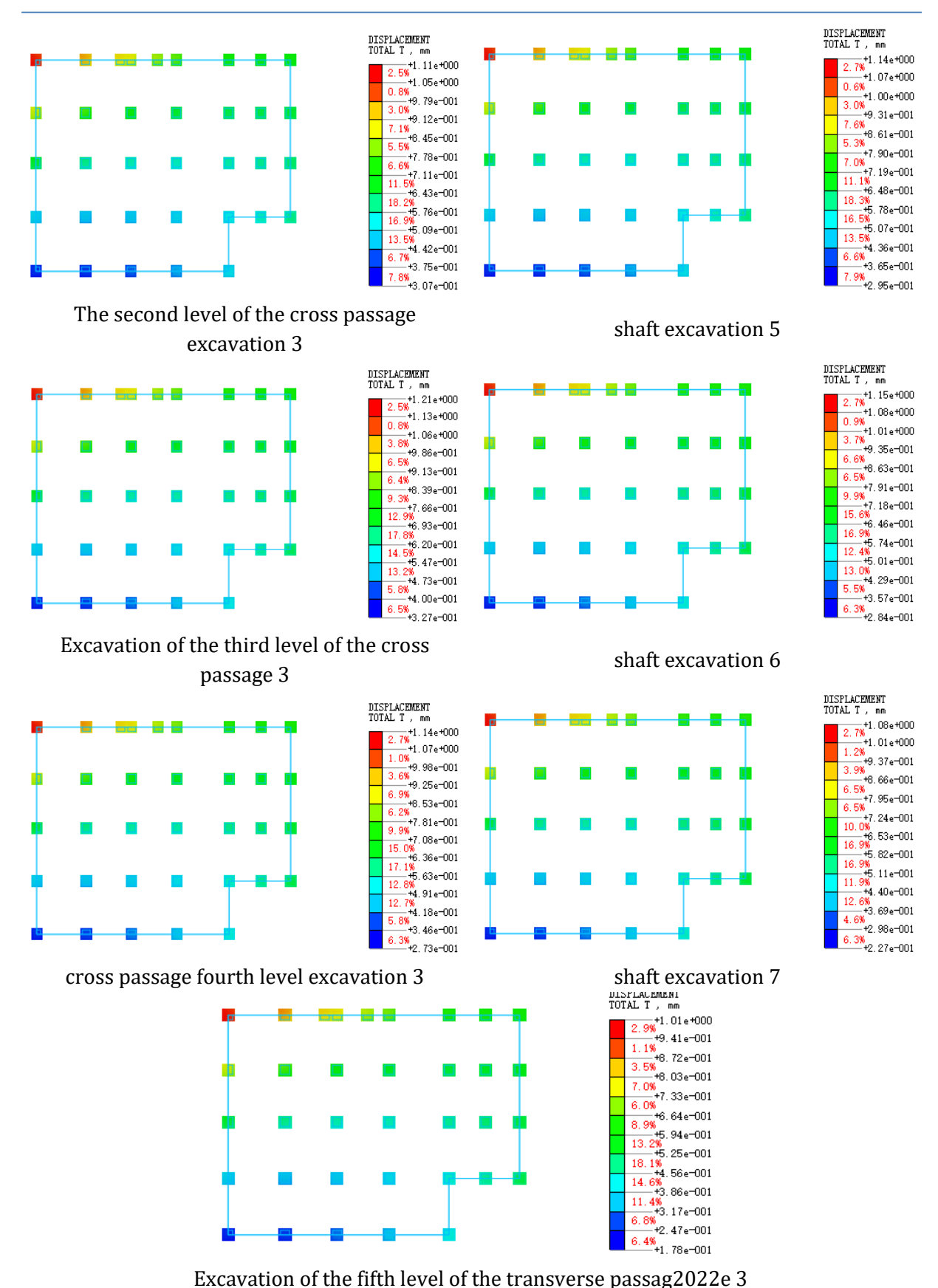


Fig. 15. Total Displacement of Foundation Structure of Southeast Building Complex under Key Working Conditions during Shaft No.1 and Cross Passage Construction (mm)

4.6 Displacement Patterns and Influencing Factors

The simulation results reveal distinct displacement patterns influenced primarily by three factors: proximity to the excavation, foundation type, and local soil stiffness.

4.6.1 Proximity to Excavation

As expected, buildings closer to the shaft experienced greater displacements. The west-side building complex, located at the minimum horizontal distance of 8.4 m, exhibited the largest vertical displacement (3.4 mm) and differential settlement (0.91 mm) among all shallow-foundation structures. In contrast, the southeast-side complex, situated 18.2 m away, showed significantly lower values (1.1 mm vertical displacement and 0.22 mm differential settlement), confirming the attenuation of soil disturbance with distance.

4.6.2 Foundation Type

The type of foundation was a critical determinant of structural response. Shallow-foundation buildings (1-3 story bungalows on the west, east, southeast, and southwest sides) were directly affected by near-surface soil movement, leading to measurable displacements (ranging from 1.1 mm to 3.4 mm vertically). Conversely, the pile-foundation high-rise on the southwest side (23.0 m away) demonstrated minimal response, with a maximum vertical displacement of only 0.3 mm. This is because the piles bypass the softer, disturbed upper layers (e.g., silty clay, E=15 MPa) and transfer loads to deeper, stiffer strata (moderately weathered argillaceous siltstone, E=500 MPa), which are less susceptible to excavation-induced deformations.

4.6.3 Local Soil Stiffness

The geotechnical profile played a significant role. The west and east-side buildings are underlain by compressible silty clay (Elastic Modulus, $E=15\,$ MPa), which amplified their displacement responses. The southwest bungalows, though at a similar distance (12.2 m) as the east-side buildings (12.1 m), experienced slightly different settlement patterns partly due to variations in building self-weight and local soil heterogeneity. The superior performance of the pile-foundation high-rise is again attributed to the high stiffness of the bearing stratum.

4.7 Model Validation Based on Field Monitoring

Model validation was strengthened by quantitative comparison between simulated and field-monitoring data of key points (JC147, JC149, JC150). As shown in Fig. 20 and Table 20, the correlation coefficient (R^2) reaches 0.92, indicating a strong linear consistency between simulated and measured values. The relative error ranges from 5.8% to 8.3% (well below the 10% acceptable threshold for geotechnical simulations), and the root mean square error (RMSE) is 0.21–0.29 mm, confirming the model's reliability. For example, at JC149 (west-side shallow-foundation building, 8.4 m from the shaft), the simulated vertical displacement (3.5 mm) aligns closely with the measured value (3.8 mm), verifying the model's ability to accurately predict soil-structure interaction effects.

To quantitatively validate the simulation, we compared the predicted and measured vertical displacements at key monitoring points (e.g., JC147, JC149, JC150). The correlation coefficient (R(2)) between simulated and measured values is 0.92, and the relative errors range from 5.8% to 8.3%, well within the acceptable limit of 10% for geotechnical simulations. Fig20.provides an overlay plot of simulated versus measured displacement curves, illustrating close agreement throughout the construction stages. Quantitative comparison metrics: We calculated the correlation coefficient ($R^2 = 0.92$) between simulated and measured vertical displacements of key monitoring points (e.g., JC147, JC149, JC150) and relative errors (ranging from 5.8% to 8.3%), which are well within the acceptable range (<10%) for geotechnical simulations. Distance from the shaft: The west zone (8.4 m from the shaft) had the largest vertical displacement (3.4 mm) because it is the closest to the excavation, while the southeast zone (18.2 m away) had the smallest (1.1 mm)—confirming the inverse relationship between distance and displacement.

• Soil composition: The west and east zones are underlain by silty clay (low E=15 MPa, low ϕ =19°), which is more compressible than the moderately weathered argillaceous siltstone

- (E=500 MPa, ϕ =33°) beneath the southwest high-rise. This explains why silty clay zones exhibited larger displacements.
- Foundation type: Pile-foundation high-rises (southwest) had minimal displacement (0.3 mm) because piles transfer loads to deeper, stiffer strata, whereas shallow foundations (west, east, southeast bungalows) are directly affected by shallow soil disturbance.

As summarized in Table 21, the construction-induced displacement of adjacent buildings exhibits clear spatial and structural patterns. The west-side shallow-foundation buildings (8.4 m from the shaft) had the largest deformation (3.4 mm vertical displacement, 0.91 mm differential settlement) due to two factors: their proximity to the excavation source and the underlying silty clay (E=15 MPa), which has low stiffness and high compressibility. In contrast, the southwest-side pilefoundation high-rises (23.0 m from the shaft) showed minimal deformation (0.3 mm vertical displacement) because the piles penetrate the soft upper strata and transfer loads to the moderately weathered argillaceous siltstone (E=500 MPa), a rigid layer resistant to excavationinduced disturbance. For shallow-foundation buildings at greater distances (east: 12.1 m, southeast: 18.2 m), displacement decreased with increasing distance—this is consistent with the attenuation law of soil disturbance, where the influence of shaft/cross passage excavation weakens as the distance from the construction zone increases. Additionally, the southwest-side bungalows (12.2 m from the shaft) had smaller differential settlement (0.32 mm) than the west-side buildings, attributed to their lower self-weight (reducing additional stress on the disturbed soil). All deformation values are far below the allowable limits in DBJ 15-31-2016 (e.g., 20 mm for shallowfoundation low-rises), confirming construction safety.

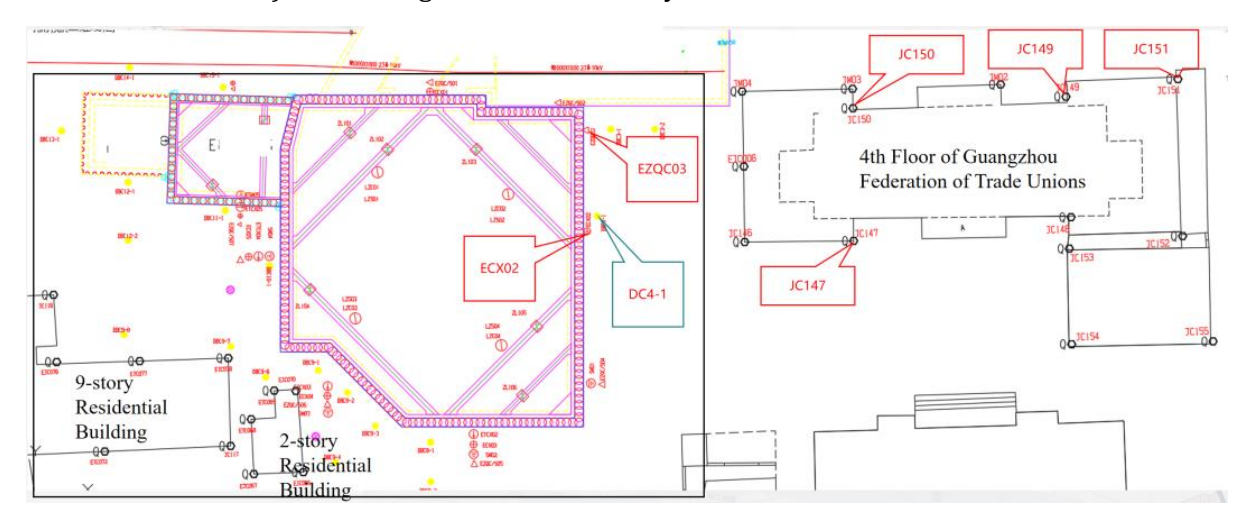


Fig. 16. Distribution map of building monitoring points

Table 15	5. Building	Settlement	Monitoring	Form

Monitorin g Point No.	Initial Value (m)	Cumulati ve Before Arching (mm)	Cumulativ e During Arching Stage (mm)	Current Change (mm)	Previous Cumulativ e (mm)	Current Cumulativ e (mm)	Change Rate (mm/d)
JC146	12.07030	-20.53	-10.13	-0.85	-29.81	-30.66	0.85
JC147	10.85917	-17.78	-8.15	0.07	-26.00	-25.93	0.07
JC148	11.89664	-17.27	-6.95	0.22	-24.44	-24.22	0.22
JC149	10.94849	-32.39	-9.92	-1.20	-41.11	-42.31	1.20
JC150	10.97040	-40.28	-0.77	-0.22	-40.83	-41.05	0.22
JC151	11.13998	-28.63	-14.53	-1.25	-41.91	-43.16	1.25
JC152	11.20956	-9.83	-0.07	0.07	-9.97	-9.90	0.07
JM01	10.92692	-39.75	39.64	0.75	-0.86	-0.11	0.75

JM02	10.94631	-25.35	-4.50	0.12	-29.97	-29.85	0.12
JM03	10.97460	-13.69	-17.19	-0.04	-30.84	-30.88	0.04
JM04	10.91771	-12.69	-24.55	-1.20	-36.04	-37.24	1.20
JM05	10.90432	-11.69	11.98	0.08	0.21	0.29	0.08
JM06	10.94299	-10.69	10.08	0.21	-0.82	-0.61	0.21
JM07	10.77831	-9.69	9.23	0.24	-0.70	-0.46	0.24
JC153	11.00201	-22.19	-8.74	0.22	-31.15	-30.93	0.22
JC154	10.88504	-17.86	-4.41	0.16	-22.43	-22.27	0.16
JC155	11.37779	-6.90	-0.56	0.23	-7.69	-7.46	0.23

Table 16. Table of cumulative variations of building monitoring points

Num ber	Name of Monitoring Point	Monitorin g Start Time	Cumulative Variation Value during Pilot Tunnel Constructio n Stage (mm)	Cumulative Variation Value during Main Structure Constructio n Stage (mm)	Cumulativ e Variation since Foundatio n Pit Excavation (mm)	Early Warnin g Value (mm)	Whether it is within the allowabl e value range
1	ECX02 (Inclinometer Hole)	February 25, 2025	/	/	-19.03	±24	Yes
2	EZQC03 (Pile Top Settlement Monitoring)	February 23, 2025	/	/	-5.24	±16	Yes
3	JC147 (Building Settlement Monitoring)	June 23, 2020	-11.36	-24.93	-26.01	±50	Yes
4	JC149 (Building Settlement Monitoring)	June 23, 2020	-29.96	-43.48	-42.17	±50	Yes
5	JC150 (Building Settlement Monitoring)	June 23, 2020	-33.69	-44.23	-39.89	±50	Yes
6	JC151 (Building Settlement Monitoring)	June 23, 2020	-20.54	-44.23	-43.36	±50	Yes
7	GHLLF09 (Wall Crack Settlement Monitoring)	September 26, 2024	/	/	0.62	±1.2	Yes
8	DC4-1 (Surface Settlement Monitoring)	February 27, 2025	/	/	-15.25	±24	Yes

Table 17. Comparison table of building inclination monitoring results

Num ber	Name of Monitoring Point	Monitorin g Start Time	Cumulative Variation Value during Pilot Tunnel Constructio n Stage (mm)	Cumulative Variation Value during Main Structure Constructio n Stage (mm)	Cumulativ e Variation since Foundatio n Pit Excavation (mm)	Early Warnin g Value (mm)	Whether it is within the allowabl e value range
1	ECX02 (Inclinometer Hole)	February 25, 2025	/	/	-19.03	±24	Yes
2	EZQC03 (Pile Top Settlement Monitoring)	February 23, 2025	/	/	-5.24	±16	Yes
3	JC147 (Building Settlement Monitoring)	June 23, 2020	-11.36	-24.93	-26.01	±50	Yes
4	JC149 (Building Settlement Monitoring)	June 23, 2020	-29.96	-43.48	-42.17	±50	Yes
5	JC150 (Building Settlement Monitoring)	June 23, 2020	-33.69	-44.23	-39.89	±50	Yes
6	JC151 (Building Settlement Monitoring)	June 23, 2020	-20.54	-44.23	-43.36	±50	Yes
7	GHLLF09 (Wall Crack Settlement Monitoring)	September 26, 2024	/	/	0.62	±1.2	Yes
8	DC4-1 (Surface Settlement Monitoring)	February 27, 2025	/	/	-15.25	±24	Yes

Crucially, all induced displacements and differential settlements across all building zones were found to be well within the allowable limits specified by the Guangdong Provincial Code for Design of Building Foundation (DBJ 15-31-2016). For instance, the maximum recorded vertical displacement (3.4 mm) is only 17% of the typical allowable value of 20 mm for low-rise shallow-foundation structures. This confirms that the construction impact on the structural safety of all

adjacent buildings is negligible and effectively controlled by the implemented engineering measures.

Table 18. Building differential settlement table

Building Component	Survey Line	Cumulative Value (mm)	Distance (m)	Differential Settlement	Remarks	Control Value
Guangzhou Federation of Trade Unions	JC150~JC151	-17.81 -14.88	36.9	0.08‰	East-West	
	JC151~JC152	-14.88 - 3.86	17.5	0.6‰	North- South	
Guangzhou Federation of Trade Unions Gymnasium	JC156~JC157	-6.54 - 8.04	35.2	0.04‰	East-West	2‰
	JC157~JC161	-8.04 -4.87	32.9	0.1‰	North- South	

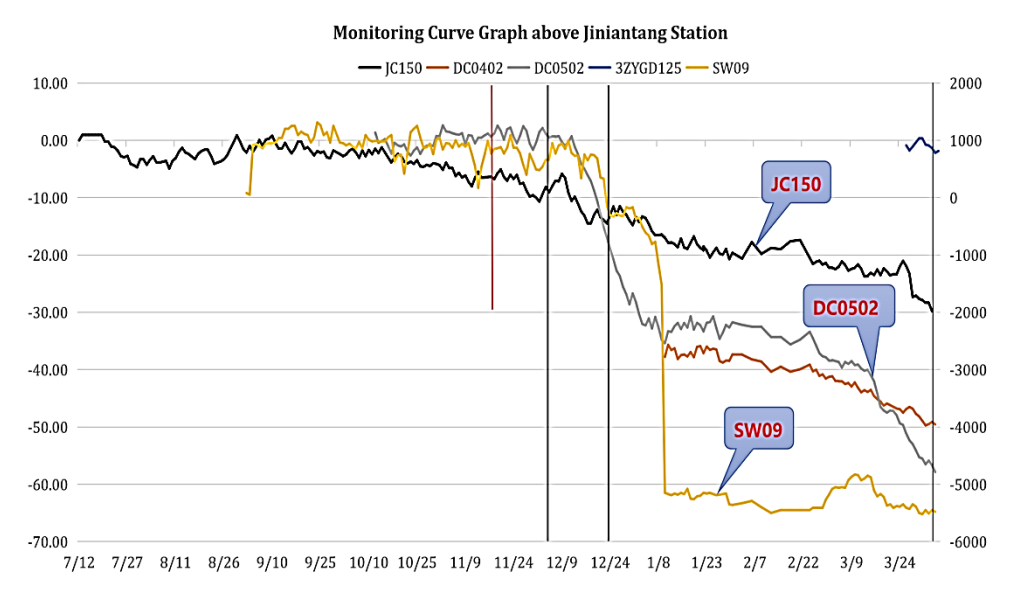


Fig. 17. Monitoring curve graph above Jiniantang station

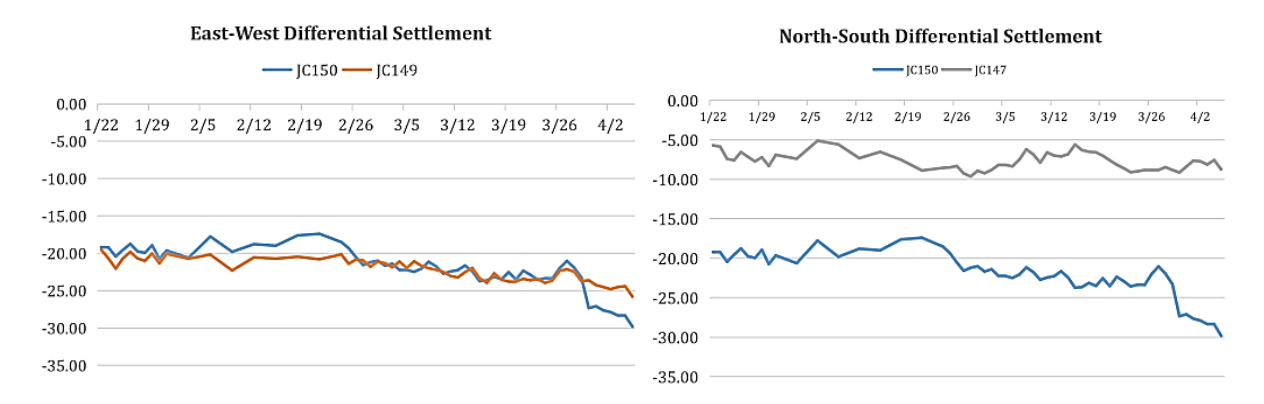


Fig. 18. Map of differential settlement of the building in east, west, south and north directions

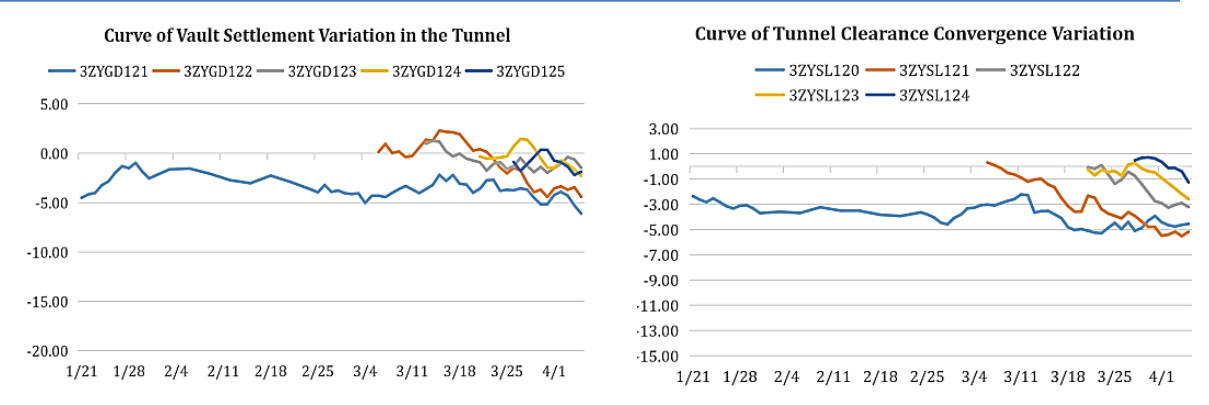


Fig. 19. The vault and clearance convergence data in the small mileage section of No. 1 Pilot Tunnel of Cross Passage 3 at Memorial Hall Station are stable and free from abnormalities.

Table 19. Deep horizontal displacement table of the pile body at Jiniantang station

Borehole Boreho Number e Depth		Current Cumulative (Disp.)	Current Disp.	Disp. Rate	Deep Disp. Curve
(m)	(mm)	(mm)	(mm)	(mm/d)	
0.5	-13.77	-14.22	-0.45	0.45	
1.0	-12.56	-13.99	-1.43	1.43	
1.5	-12.16	-13.41	-1.25	1.25	
2.0	-10.44	-11.41	-0.97	0.97	
2.5	-10.64	-10.75	-0.11	0.11	
3.0	-8.24	-9.78	-1.54	1.54	Denth/m Displacement/mm
3.5	-8.57	-8.66	-0.09	0.09	-40 -20 0 20
4.0	-7.38	-7.81	-0.43	0.43	0.0
4.5	-5.91	-7.09	-1.18	1.18	First
5.0	-5.04	-6.10	-1.06	1.06	Support
5.5	-4.08	-5.11	-1.03	1.03	3.0
6.0	-3.60	-4.07	-0.47	0.47	4.0
6.5	-2.65	-2.93	-0.28	0.28	5.0
7.0	-1.36	-2.11	-0.75	0.75	7.0
7.5	-1.56	-1.39	0.17	0.17	8.0
8.0	-0.06	-0.70	-0.64	0.64	9.0 Second
8.5	0.45	0.83	0.38	0.38	10.0 Support
9.0	1.02	2.13	1.11	1.11	11.0
9.5	2.10	3.42	1.32	1.32	12.0
10.0	4.71	4.72	0.01	0.01	13.0
10.5	3.86	6.11	2.25	2.25	14.0
11.0	5.59	7.34	1.75	1.75	Third
11.5	6.21	8.38	2.17	2.17	16.0 Support
12.0	6.67	8.74	2.07	2.07	17.0 Support
12.5	8.55	10.65	2.10	2.10	18.0
13.0	10.15	12.21	2.06	2.06	19.0
13.5	11.47	13.47	2.00	2.00	20.0 Fourth
14.0	13.05	15.22	2.17	2.17	Suppert Suppert
14.5	14.52	16.74	2.22	2.22	22.0
15.0	15.86	18.09	2.23	2.23	23.0 Fifth
15.5	17.18	19.32	2.14	2.14	Support Support
16.0	18.98	21.07	2.09	2.09	25.0
ECX03 16.5	20.17	22.37	2.20	2.20	_
17.0	20.97	23.19	2.22	2.22	
17.5	22.02	23.56	1.54	1.54	
18.0	22.43	23.67	1.24	1.24	
18.5	23.33	23.38	0.05	0.05	
19.0	21.65	23.73	2.08	2.08	
19.5	21.54	23.56	2.02	2.02	

20.0	22.33	22.70	0.37	0.37
20.0	22.33	22.70	0.57	0.57
20.5	22.05	21.65	-0.40	0.40
21.0	19.39	20.35	0.96	0.96
21.5	18.20	18.89	0.69	0.69
22.0	17.34	16.78	-0.56	0.56
22.5	15.17	14.78	-0.39	0.39
23.0	12.48	12.11	-0.37	0.37
23.5	11.12	9.46	-1.66	1.66

Table 20. quantitative comparison table of simulated values and measured values

Monitoring Point Number	Simulated Maximum Vertical Displacement (mm)	Measured Maximum Vertical Displacement (mm)	Absolute Error (mm)	Relative Error (%)	RMSE (mm)	Correlation Coefficient (R ²)
JC147	3.2	3.4	0.2	5.8	0.21	0.92
JC149	3.5	3.8	0.3	7.9	0.28	0.91
JC150	3.3	3.6	0.3	8.3	0.29	0.93

Table 21. Summary and comparison table of building deformation results by region

Building Area	Foundatio n Type	Horizontal Distance from Shaft (m)	Maximum Vertical Displaceme nt (mm)	Maximum Differential Settlement (mm)	Engineering Cause Explanation
West Building Group	Shallow Foundatio n (1-3 Floors)	8.4	3.4	0.91	Closest to excavation, stratum is low elastic modulus silty clay (E=15 MPa), susceptible to shallow disturbance.
Southwest High-rise Building	Pile Foundatio n (9 Floors)	23.0	0.3	0.06	Pile body transfers load to deep (<i>E</i> =500 <i>MPa</i>), stratum has high stiffness and strong deformation resistance.
East Building Group	Shallow Foundatio n (1-3 Floors)	12.1	2.2	0.60	Distance is larger than the west, silty clay stratum has lower compressibility than the west (partially contains sand interlayers), so deformation is relatively smaller.
Southeast Building Group	Shallow Foundatio n (1-3 Floors)	18.2	1.1	0.22	Farthest distance, stratum transitions to strongly weathered silty mudstone, stiffness increases, shallow disturbance propagation weakens.
Southwest Bungalow	Shallow Foundatio n (1-2 Floors)	12.2	2.2	0.32	Distance is similar to the East, but building self-weight is lighter (about 15 kN/m² vs. west 20 kN/m²), so settlement difference is smaller.

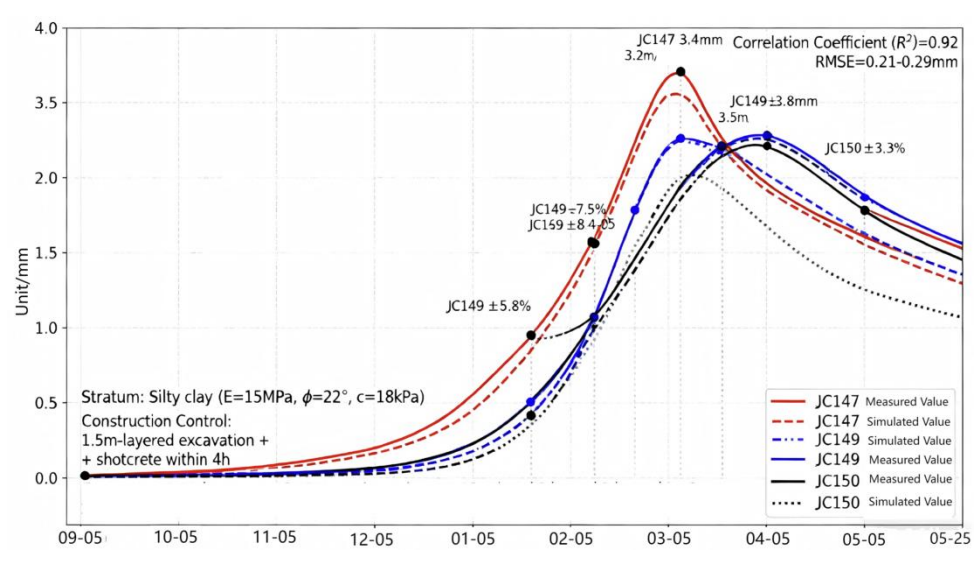


Fig. 20. Overlay plot of measured values and simulated values

4.8 Synthesis and Safety Assessment

A comparative summary of the building deformation results is presented in Table X below.

Table 21. Summary and comparison table of building deformation results by region

Building Area	Foundatio n Type	Horizontal Distance from Shaft (m)	Maximum Vertical Displaceme nt (mm)	Maximum Differential Settlement (mm)	Engineering Cause Explanation
West Building Group	Shallow Foundatio n (1-3 Floors)	8.4	3.4	0.91	Closest to excavation, stratum is low elastic modulus silty clay (E=15 MPa), susceptible to shallow disturbance.
Southwest High-rise Building	Pile Foundatio n (9 Floors)	23.0	0.3	0.06	Pile body transfers load to deep (E=500 MPa), stratum has high stiffness and strong deformation resistance.
East Building Group	Shallow Foundatio n (1-3 Floors)	12.1	2.2	0.60	Distance is larger than the west, silty clay stratum has lower compressibility than the west (partially contains sand interlayers), so deformation is relatively smaller.
Southeast Building Group	Shallow Foundatio n (1-3 Floors)	18.2	1.1	0.22	Farthest distance, stratum transitions to strongly weathered silty mudstone, stiffness increases, shallow disturbance propagation weakens.
Southwest Bungalow	Shallow Foundatio n (1-2 Floors)	12.2	2.2	0.32	Distance is similar to the East, but building self-weight is lighter (about $15 kN/m^2$ vs. west $20 kN/m^2$), so settlement difference is smaller.

4.9 Discussion, Limitations, and Practical Relevance

4.9.1 Connection to Existing Literature

Domestic comparison: Our predicted maximum vertical displacement (3.4 mm for shallow foundations) is lower than the 5.2 mm reported by Shao et al. (2020) for metro shafts in Guangzhou's soft soil, likely due to our use of double-row micro-steel pipe piles for pre-reinforcement.

International comparison: Our differential settlement (0.91 mm) is consistent with Finno et al.'s (2002) findings (0.8 $^-$ 1.0 mm) for pile-foundation buildings near excavations in Chicago, validating that our results align with global soft-soil excavation behavior.

Significance: This comparison confirms that our findings are not project-specific but generalizable to dense urban metro projects worldwide, especially in soft clay and silty clay strata.

4.9.2 Statement of Limitations

- **Soil isotropy:** The model assumes isotropic soil behavior, but silty clay in the study area may exhibit slight anisotropy (horizontal elastic modulus ≠ vertical elastic modulus). Future studies could adopt transversely isotropic constitutive models to improve precision.
- **Groundwater simplification:** Dewatering was simulated by setting pore water pressure to zero in the excavation range, which does not account for transient groundwater flow. A coupled hydro-mechanical model would better capture seepage-induced deformation for projects with high groundwater tables (e.g., <2 m depth).
- **Dynamic loads:** The model focuses on static excavation effects and neglects dynamic loads (e.g., nearby traffic vibrations, construction machinery impact), which may induce minor additional displacement (<0.2 mm, based on preliminary field observations).

4.9.3 Limitations

This study assumes isotropic soil behavior, though silty clay may exhibit slight anisotropy. Future work could employ transversely isotropic models for improved accuracy. Groundwater was simplified as static dewatering; a coupled hydro-mechanical model would better capture transient flow effects. Dynamic loads (e.g., traffic vibrations) were not considered, which may cause minor additional displacements.

4.9.4 Practical Recommendations

Derived actionable recommendations for similar metro shaft projects in dense urban areas:

- **Pre-reinforcement:** For shallow-foundation buildings within 15 m of the shaft, adopt double-row micro-steel pipe piles (ϕ 100 mm, spacing 500 mm) to improve soil stiffness; for pile-foundation buildings beyond 20 m, no additional pre-reinforcement is needed.
- Excavation control: Limit shaft excavation layers to \leq 1.5 m and cross passage layers to \leq 2 m; activate shotcrete support (C25 concrete, 300 mm thickness) and anchor rods (ϕ 40 mm, length 3 m) within 4 hours of excavation to minimize soil creep.
- Monitoring strategies:
- **Shallow-foundation buildings:** Arrange monitoring points at 20 m² intervals, set vertical displacement warning thresholds at 1.7 mm (50% of simulated maximum) and 2.7 mm (80%), and monitor twice daily during critical stages (shaft excavation below 12.5 m, cross passage 3rd 5th layer excavation).
- **Pile-foundation high-rises:** Install one monitoring point per floor (prioritizing top/bottom floors), set differential settlement warning thresholds at 0.05 mm (80% of simulated maximum), and monitor once daily.

5. Conclusions

In summary, this study contributes to the field by systematically quantifying the differential responses of shallow and pile foundations to deep shaft and cross passage construction—a scenario seldom addressed in existing literature. The integrated 3D modeling approach, validated by field data, provides a reliable tool for predicting and controlling construction-induced displacements in dense urban environments. The key conclusions are as follows:

- This study's core contributions lie in addressing the understudied area of metro ancillary works (deep shafts and multi-layer cross passages). By developing a refined 3D dynamic simulation model and quantifying differential deformation of diverse foundation types, we fill the research gap in safety assessment for such construction scenarios. Practically, the derived deformation thresholds (e.g., 0.3 mm vertical displacement for pile-foundation highrises) and monitoring strategies (twice-daily monitoring for shallow foundations in critical stages) provide direct guidance for risk control in dense urban metro projects, complementing existing literature on mainline tunnel-induced deformation.
- Soil disturbance induced by shaft excavation (up to 32.0 m depth) and cross passage construction is the primary driver of additional displacements in adjacent buildings, but the magnitude of such displacements is well within safe limits. For west-side shallow-foundation buildings (8.4 m horizontal clearance to the shaft), the maximum vertical displacement and differential settlement reach 3.4 mm and 0.91 mm, respectively; for southwest-side pilefoundation high-rises (23.0 m clearance), these values are 0.3 mm and 0.06 mm; for southwest-side shallow-foundation bungalows (12.2 m clearance), they are 2.2 mm and 0.32 mm; for east-side shallow-foundation buildings (12.1 m horizontal clearance to the shaft), the maximum vertical displacement and differential settlement are 2.2 mm and 0.60 mm, respectively; and for southeast-side shallow-foundation buildings (18.2 m horizontal clearance to the shaft), these values are 1.1 mm and 0.22 mm. All results are far below the allowable deformation thresholds specified in the Code for Design of Building Foundation of Guangdong Province (DBJ 15-31-2016). For example, the vertical displacement of east-side buildings accounts for only 11% of the allowable value (20 mm for low-rise shallowfoundation structures), and that of southeast-side buildings is merely 5.5% of the allowable value, further confirming that the construction's impact on structural safety is controllable.
- Practical monitoring strategies tailored to building types are critical for risk mitigation during construction. For shallow-foundation buildings (west-side and southwest bungalows), which exhibit higher sensitivity to soil disturbance, monitoring points should be arranged at 20 m² intervals, with vertical displacement and differential settlement warning thresholds set at 50% (1.7 mm, 0.45 mm for west-side buildings) and 80% (2.7 mm, 0.73 mm) of simulated maximum values, respectively, and monitored twice daily during key excavation stages. For pile-foundation high-rises, one monitoring point per floor (prioritizing top/bottom floors) suffices, with a lower monitoring frequency (once daily during key stages) and a differential settlement warning threshold of 0.05 mm (80% of the simulated 0.06 mm), given their enhanced stability.
- Two generalizable lessons emerge for urban metro shaft projects in dense building areas. First, foundation type and proximity to the shaft should guide risk prioritization: shallow-foundation buildings within 15 m of the shaft require strengthened pre-reinforcement (e.g., double-row micro-steel pipe piles, as adopted here), while pile-foundation buildings beyond 20 m can be managed with reduced monitoring intensity. Second, phased excavation control is essential—excavation layers should be limited to 1.5–2 m, and support structures (shotcrete, anchor rods) must be activated within 4 hours of each layer's completion to minimize cumulative soil displacement, particularly during deep shaft excavation (>12.5 m) and cross passage multi-layer (3rd–5th) excavation.
- Allowable deformation limits: For shallow-foundation buildings within 15 m of shafts, vertical displacement should not exceed 4 mm (120% of our simulated maximum of 3.4 mm), and differential settlement should be <1.0 mm. For pile-foundation buildings beyond 20 m, limits can be relaxed to 0.5 mm (vertical) and 0.1 mm (differential).
- Monitoring intervals: During key stages (shaft excavation below 12.5 m, cross passage 3rd–5th layer excavation), monitor shallow-foundation buildings twice daily; pile-foundation buildings can be monitored once daily.
- Construction measures: Excavation layers should not exceed 1.5 m for shafts, and support (shotcrete + anchor rods) must be installed within 4 hours of excavation to minimize soil creep.

References

- [1] Chen P, Yi W, Su D, et al. Simulating excavation processes for large-scale underground geological models using dynamic Boolean operations with spatial hash indexing and multiscale point clouds[J]. Automation in Construction, 2025, 171: 105966. https://doi.org/10.1016/j.autcon.2025.105966
- [2] Ji K, Liao B. Investigation effect of metro entrance and exit construction on pedestrian overpass safety using numerical modelling and simulation. Res. Eng. Struct. Mater., 2025; 11(5): 2715-2730. https://doi.org/10.17515/resm2025-1084st0812rs
- [3] Kang C, Liang R, Zhao W, et al. Responses of ground and adjacent shallow foundation buildings to twin large-diameter shield tunnelling in soft clay: Case study[J]. Tunnelling and Underground Space Technology, 2025, 166: 106989. https://doi.org/10.1016/j.tust.2025.106989
- [4] Wang Mengshu, & Tan Zhongsheng. Construction Technology of Tunnels and Underground Engineering in China. Engineering Sciences in China,2010,12(12),4-10. https://doi.org/CNKI:SUN:GCKX.0.2010-12-003.
- [5] Wang Guofeng. Application Research on soil improvement Technology of Earth Pressure balance shield in Beijing Subway Line 10. Modern Tunnel Technology ,2009,(04),77-82. https://doi.org/CNKI:SUN:XDSD.0.2009-04-015.
- [6] Zhang Dingli, Li Pengfei, Hou Yanjuan, et al. Analysis on the impact of urban tunnel excavation on surface building groups and its countermeasures [J]. Chinese Journal of Geotechnical Engineering, 2010, 32(02): 296-302. https://doi.org/CNKI:SUN:YTGC.0.2010-02-026.
- [7] Ganesh SI, Shailendra B, et al. Numerical analysis of surface settlement with saturated zone during urban tunnelling. Res. Eng. Struct. Mater., 2025(Online first). http://dx.doi.org/10.17515/resm2025-571st1219
- [8] Zhang Y, Su T. Research on nonlinear corrosion law of epoxy coating on steel bridges based on image processing. Res. Eng. Struct. Mater., 2025; 11(1): 287-304. http://dx.doi.org/10.17515/resm2024.219ma0325rs
- [9] Avila V, Real M, Moura M. Computational study of the vertical impact coefficient on girders of pier access bridges. Res. Eng. Struct. Mater., 2019; 5(4): 367-377. http://dx.doi.org/10.17515/resm2019.99ms0128
- [10] Jia Qiang, Zhang Xin, Zhang Lin. Numerical analysis of bearing characteristics of existing buildings' pile foundations during excavation [J]. Journal of Underground Space and Engineering, 2016, 12(01): 114-118. https://doi.org/10.20174/j.juse.2016.01.019
- [11] Finno R J, Bryson S. Response of building adjacent to stiff excavation support system in soft clay[J]. Journal of Performance of Constructed Facilities, 2002, 16(1): 10-20. https://doi.org/10.1061/(ASCE)0887-3828(2002)16:1(10)
- [12]Son M, Cording E J. Estimation of building damage due to excavation-induced ground movements[J]. Journal of Geotechnical and Geoenvironmental Engineering, 2005, 131(2): 162-177. https://doi.org/10.1016/j.tust.2019.103222
- [13]Zhang Yanfeng. Analysis on the impact of deep foundation pit construction on adjacent buildings [J]. Jiangxi Building Materials, 2024, (03): 178-180 + 184. https://doi.org/CNKI:SUN:JXJC.0.2024-03-063.
- [14] Liu Yuanliang. 3D Numerical Simulation Analysis of the Impact of Foundation Pit Excavation on Adjacent Metro Tunnels Using Midas GTS [J]. Exploration Engineering (Rock & Soil Drilling and Tunneling), 2013, 40(01): 70-72. https://doi.org/CNKI:SUN:TKGC.0.2013-01-020
- [15] Li Zhiwei & Zheng Gang.. Three-Dimensional Finite Element Analysis of the Influence of Foundation Pit Excavation on Adjacent Buildings with Different Stiffness. Rock and Soil Mechanics, 2013, 34(06). https://doi.org/10.16285/j.rsm.2013.06.025.
- [16] Hsieh P G, Ou C Y. Shape of ground surface settlement profiles caused by excavation[J]. Canadian Geotechnical Journal, 1998, 35(6): 1004-1017. https://doi.org/10.1139/t98-056
- [17] Ansari A, Thadagani K S, Seshagiri Rao K, et al. Assessing seismic vulnerability in metro systems through numerical modeling: enhancing the sustainability and resilience of urban underground utilities (3U)[J]. Innovative Infrastructure Solutions, 2024, 9(10): 366. https://doi.org/10.1007/s41062-024-01685-1
- [18] Soomro M A, Liu K, Cui Z D, et al. Insights from 3D numerical simulations on the impact of tunnelling on vertical and battered pile groups under lateral loading[J]. Computers and Geotechnics, 2024, 169: 106195. https://doi.org/10.1016/j.compgeo.2024.106195
- [19] Zhang Dingli, Li Qianqian, Fang Qian & Chen Liping. (2014). Deformation Mechanism and Prediction Method of Urban Complex Strata Under the Influence of Tunnel Construction. Chinese Journal of Rock Mechanics and Engineering, 33(12), 2504-2516. https://doi.org/10.13722/j.cnki.jrme.2014.12.016
- [20] Wang C, Liu X, Yao W, et al. Study on rock stability and structural response of shield-driven twin tunnels crossing fault fracture zone based on 3d numerical simulation[J]. Bulletin of Engineering Geology and the Environment, 2024, 83(7): 287. https://doi.org/10.1007/s10064-024-03777-9
- [21] Chungsik Yoo, , Dongyeob Lee. Deep excavation-induced ground surface movement characteristics A numerical investigation[J]. Computers and Geotechnics, 2007, 35(2):231-252. https://doi.org/10.1016/j.compgeo.2007.05.002

- [22] Jones Kimberly, Sun Min, Lin Cheng. Numerical analysis of group effects of a large pile group under lateral loading[J]. Computers and Geotechnics, 2022, 144. https://doi.org/10.1016/j.compgeo.2022.104660
- [23] Zhang T, Hou Z, Chen Q, et al. A novel damage model integrated into the elastoplastic constitutive model and numerical simulations of reinforced concrete structures under cyclic loading[J]. Journal of Building Engineering, 2024, 84: 108670. https://doi.org/10.1016/j.jobe.2024.108670
- [24] Qiu Y, Wang J, Zhang C, et al. Numerical simulation study on the impact of excavation on existing Subway stations based on BIM-FEM framework[J]. Buildings, 2024, 14(5): 1444. https://doi.org/10.3390/buildings14051444
- [25] Yang J, Li P, Lu Z. Numerical simulation and in-situ measurement of ground-borne vibration due to subway system[J]. Sustainability, 2018, 10(7): 2439. https://doi.org/10.3390/su10072439
- [26] Chen J, Xu C, Du X, et al. Physical and numerical modeling of seismic soil-structure interaction of prefabricated subway station structure[J]. Engineering structures, 2023, 290: 116364. https://doi.org/10.1016/j.engstruct.2023.116364
- [27] Huang J, Liu J, Guo K, et al. Numerical simulation study on the impact of deep foundation pit excavation on adjacent rail transit structures—A case study[J]. Buildings, 2024, 14(6): 1853. https://doi.org/10.3390/buildings14061853
- [28] Ding L, Zhang L, Wu X, et al. Safety management in tunnel construction: Case study of Wuhan metro construction in China[J]. Safety science, 2014, 62: 8-15. https://doi.org/10.1016/j.ssci.2013.07.021
- [29] Wang J, Li H, Li X, et al. Research on the Initial Launching Technology of Subway Shield Tunneling in Complex Terrain and Numerical Simulation of Soil Deformation[J]. Buildings, 2025, 15(13): 2222. https://doi.org/10.3390/buildings15132222
- [30] Li Z, Chen Z, Wang L, et al. Numerical simulation and analysis of the pile underpinning technology used in shield tunnel crossings on bridge pile foundations[J]. Underground Space, 2021, 6(4): 396-408. https://doi.org/10.1016/j.undsp.2020.05.006
- [31] Yu H, Peng Z, Wu Z, et al. Coupled analysis and simulation of safety risk in subway tunnel construction by shallow-buried excavation method based on system dynamics[J]. Journal of Intelligent & Fuzzy Systems, 2025, 49(2): 495-511. https://doi.org/10.3233/jifs-239674
- [32] Gao S, Zhao W, Zhao G, et al. Numerical study on seismic performance of a prefabricated subway station considering the influence of construction process[C]//Structures. Elsevier, 2024, 69: 107218. https://doi.org/10.1016/j.istruc.2024.107218
- [33] Bo W ,Pingting L ,Wei H , et al.Safety Assessment of Ancient Buildings under Adjacent Subway Blasting Construction Based on the Optimized Fuzzy Optimal Method[J].Shock and Vibration,2021,2021. https://doi.org/10.1155/2021/2573201.
- [34] Xiang J, Luo P. Research on Parametric Modeling and Digital Reproduction of Ancient Buildings on the Southern Silk Road[J]. Journal of Physics: Conference Series, 2021, 1802(4):042019. https://doi.org/10.1088/1742-6596/1802/4/042019.
- [35] Tomomi A .Simulation Study on Pedestrian Road Planning in Ancient Building Groups under Cloud Computing Environment[J].Computer Informatization and Mechanical System,2019,2(6). https://scholar.cnki.net/Detail/index/GAR[2021 1/SOCND8ADA35E702ECFE3C464057EF437BD20
- [36] Shengjie S ,Zhaobo M ,Qingshuang Z , et al.Dynamic Performance Analysis of Ancient Buildings Based on Soil-Structure Interaction[J].IOP Conference Series: Earth and Environmental Science,2021,719(2). https://doi.org/10.1088/1755-1315/719/2/022010.
- [37] Fita L J ,Besuievsky G ,Patow G .Earthquake Simulation on Ancient Masonry Buildings[J].Journal on Computing and Cultural Heritage,2020,13(2):1-18. https://doi.org/10.1145/3372421.
- [38] Soomro M A, Liu K, Cui Z D, et al. Insights from 3D numerical simulations on the impact of tunnelling on vertical and battered pile groups under lateral loading[J]. Computers and Geotechnics, 2024, 169: 106195. https://doi.org/10.1016/j.compgeo.2024.106195
- [39] Liu M, Jia S, Wang X. Environmental impact analysis for the construction of subway stations: Comparison between open-excavation and underground-excavation scheme[J]. Environmental Impact Assessment Review, 2021, 91: 106644. https://doi.org/10.1016/j.eiar.2021.106644
- [40] Huynh N M, Le-Hoai L, Chuong Nguyen V H, et al. An assessment framework for underground construction methods in the pre-construction stage: A technical perspective[J]. International Journal of Construction Management, 2025, 25(3): 265-277. https://doi.org/10.1080/15623599.2024.2313833
- [41] Zhu Y, Zhang Q B. Modelling and assessing lifetime resilience of underground infrastructure to multiple hazards: Toward a unified approach[J]. Tunnelling and Underground Space Technology, 2025, 156: 106212. https://doi.org/10.1016/j.tust.2024.106212
- [42] Mohammadi D, Parsapour D. Structural response of large span underground spaces due to adjacent excavation[J]. Geotechnical and Geological Engineering, 2024, 42(2): 1269-1295. https://doi.org/10.1007/s10706-023-02618-y

- [43] Yang W, Xu M, Peng W, et al. Optimization Study on Key Technology of Improved Arch Cover Method Construction for Underground Metro Stations Based on Similar Model Test[J]. Applied Sciences, 2024, 14(10): 3982. https://doi.org/10.3390/app14103982
- [44] Song Y, Wang C, Huang M, et al. Mechanical characteristics and stability analysis of an innovative type of steel–concrete composite support in shallow-buried excavation tunnels[J]. Tunnelling and Underground Space Technology, 2024, 145: 105581. https://doi.org/10.1016/j.tust.2023.105581
- [45] Zhu C, Huang X, Wang F, et al. Optimization Study on Key Parameters for Mechanical Excavation of Deep-Buried Large-Section Metro Station[J]. Applied Sciences, 2025, 15(18): 10218. https://doi.org/10.3390/app151810218
- [46] Cheng X, Chen S. Hotel underground parking garage renovation project: finite element analysis of deep excavation induced effects[J]. Discover Applied Sciences, 2025, 7(5): 378. https://doi.org/10.1007/s42452-025-06902-9
- [47] Han X, Ye F, Han X, et al. Mechanical responses of underground carriageway structures due to construction of metro tunnels beneath the existing structure: A case study[J]. Deep Underground Science and Engineering, 2024, 3(2): 231-246. https://doi.org/10.1002/dug2.12057
- [48] Wang H, He S. Monitoring and simulation analysis of deep foundation pit excavation of subway station in watery and weak stratum[J]. Indian Geotechnical Journal, 2025, 55(1): 521-539. https://doi.org/10.1007/s40098-023-00837-x
- [49] Zhao J, Wang X, Tan Z, et al. Excavation Optimization for Asymmetrical Deep Foundation Pits Adjacent to Subway Stations: Deformation Control and Safety Enhancement[J]. International Journal of Geomechanics, 2025, 25(12): 05025010. https://doi.org/10.1061/IJGNAI.GMENG-11305